Marine Structures 101 (2025) 103763

Contents lists available at ScienceDirect

Marine Structures

journal homepage: www.elsevier.com/locate/marstruc

Review article

Methods for the local mechanical analysis of submarine power cables: A systematic literature review

Pan Fang [a,*], Xiao Li [b,*], Xiaoli Jiang [a], Hans Hopman [a], Yong Bai [c]

[a] Department of Maritime and Transport Technology, Delft University of Technology, Netherlands
[b] Institute of High Performance Computing (IHPC), Agency for Science, Technology and Research (A*STAR), 1 Fusionopolis Way, #16-16 Connexis, Singapore 138632, Republic of Singapore
[c] College of Civil Engineering and Architecture, Zhejiang University, Hangzhou, Zhejiang, PR China

ARTICLE INFO

Keywords:
Submarine power cables
Local mechanical analysis
Tension
Bending
Experimental
Analytical
Numerical

ABSTRACT

As the wind industry expands into remoter and deeper areas of the open sea with abundant wind energy, environmental loadings become harsher. This increases the requirements for submarine power cables (SPCs), which serve as the 'lifeline' for transporting electricity. Consequently, a more advanced design based on a thorough understanding of this structure is needed. However, the complex configuration and intensive contact issues within SPCs limit our understanding and make them black boxes for cable engineers. To gain more insights, methods for performing local mechanical analysis of SPCs are necessary. Despite this need, a comprehensive review of existing methods for local mechanical analysis of SPC is still lacking. Therefore, it is essential to review the available methods and provide guidelines for utilizing and developing these methods.

Contents

* Corresponding authors.
E-mail addresses: P.Fang-1@tudelft.nl (P. Fang), li_xiao@ihpc.a-star.edu.sg (X. Li).

https://doi.org/10.1016/j.marstruc.2024.103763
Received 17 May 2024; Received in revised form 4 August 2024; Accepted 10 December 2024

Nomenclature

α	Winding angle of helical components
E	Young's Modulus
V	Angular position
t	Thickness
b	Width
A	Cross section area
p	Pitch length
n	Number of helix in current layer
K	Stiffness
δ	Axial strain
σ	Stress
ε	Strain
P	Pressure
N	Tension
M	Moment
φ	Torsion angle
f	Friction force
μ	Friction coefficient
θ	Bending angle
k	Curvature
D	Diameter
u	Displacement
GJ	Torsion stiffness
T	Torque
τ	Torsion angle per unit length

1. Introduction

Over the past few decades, there have been significant advancements in offshore energy production technologies, including floating offshore wind farms and wave energy converter systems. Among these, wind energy has proven particularly promising, garnering increasing attention in the academic and industrial sectors [1–4]. Recent years have witnessed robust growth in offshore wind energy, a trend that is projected to continue, as depicted in Fig. 1. In 2024, global offshore wind capacity is estimated at nearly 70 Gigawatts [5]. Specifically, in Europe, there are more than 100 offshore wind farm installations across eleven countries, boasting a combined capacity of approximately 23 Gigawatts [6].

A key strategy for harnessing significant wind energy involves exploiting more distant oceanic areas, where winds are plentiful. As Europe targets climate neutrality by 2050, achieving this goal requires the development of up to 150 GW of floating offshore wind capacity [7]. Fig. 2 illustrates this ongoing trend within the North Sea basin.

Wind farms are comprised of turbines dedicated to transforming wind energy into electricity. Fig. 3 highlights a crucial element within these farms: submarine power cables (SPCs). Acting as the vital "lifeline", these cables are responsible for transmitting the electricity generated by wind turbines to consumers. The history of power cables extends over a century [10], though initially, they were confined to terrestrial and overhead uses. However, they eventually transitioned into maritime settings, adapting their structural designs to meet the evolving demands of the industry [11].

Each cable is intricately customized to suit its specific role and project, leading to continuous evolution in its configuration and internal components, which may vary from one project to another. From a mechanical perspective, a cable comprises four main components: conductor, insulation system, armour wire, and serving, as detailed in Table 1, which lists their materials and functions. For a multi-core SPC, such as the three-core SPC in Fig. 4(b), there could also be extra components, e.g., fillers. Additionally, thin screens or tapes exist among each main layer.

In the design of SPCs, strength and flexibility are paramount concerns from a mechanical perspective [15]. To ensure strength, sufficient metals are incorporated within the SPC, while flexibility is achieved by designing some internal components into a helical shape [16]. These helical components are intended to mitigate built-up stress during loading by permitting the components to move

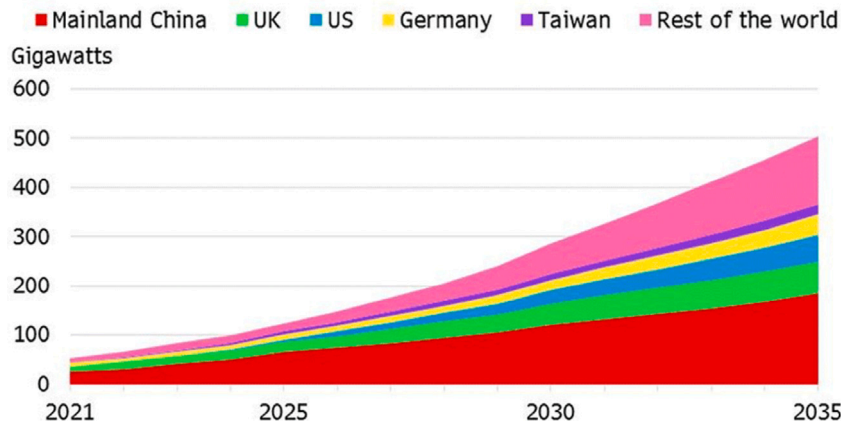

Fig. 1. Cumulative offshore wind capacity around the world [8].

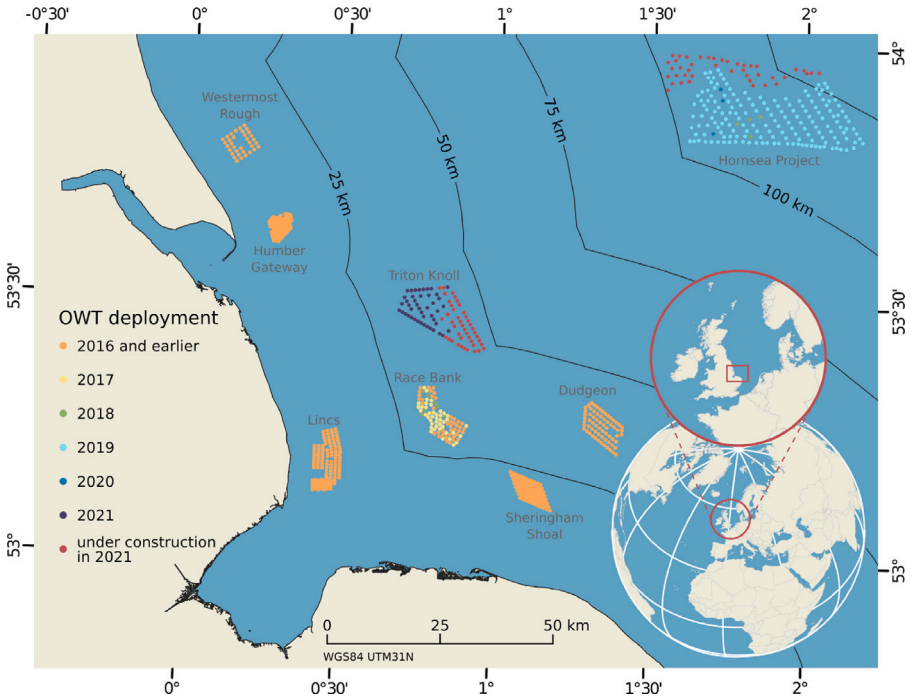

Fig. 2. Offshore wind farms and their locations at the East England coast in the North Sea Basin [9].

Table 1
Main components inside a cable.

Component	Material	Function
Conductor	Copper/Aluminium	Electricity transportation
Insulation	Cross-linked polyethene	Prevent electrical leakage
Armour	Steel	Provide mechanical protection
Serving	Polymer	Anti-corrosion

apart. Although this design extends cables' lifespan, it also increases complexity and renders SPCs less comparable to the other flexible structures used in oil and gas industry, such as flexible pipes and umbilicals.

A typical flexible pipe, shown in Fig. 5(b), primarily designed to transport oil and gas, features a hollow centre to allow fluid flow. Unlike SPCs, the armour layers of a flexible pipe often consist of helical wires with rectangular cross-sections. An umbilical, shown in Fig. 5(c), resembles more SPCs. However, the inner components in an umbilical distinguish significantly from SPCs. Particularly,

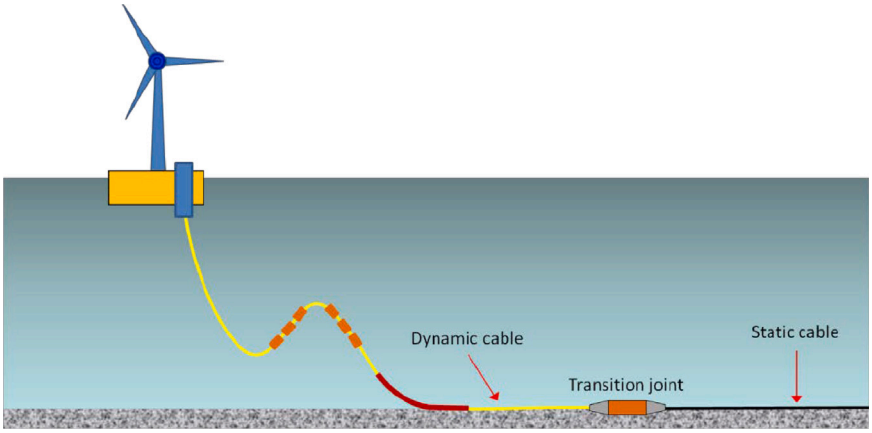

Fig. 3. Facilities in floating wind system [12].

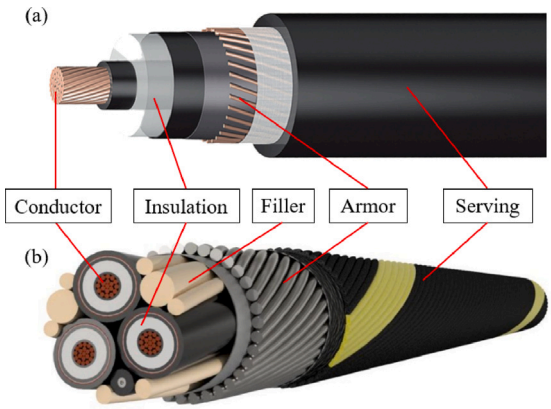

Fig. 4. Typical configuration of a one-core SPC (a) [13] and a three-core SPC (b) [14].

SPCs contain numerous large-size metal components that play a significant role in determining the ultimate performance. This issue has not been paid much attention to in the previous studies regarding both flexible pipes and umbilicals.

The special structure configuration distinguishes the local behaviours of SPCs from other flexible structures and an inappropriate design can cause failures that were not observed in flexible pipes. Electrical tree and water tree [19,20] due to large deformation, for example, are possible mechanism causing the failure in the insulation for SPCs; Fatigue failure of copper conductors is also an example [21–23]. Therefore, a better understanding of the local mechanical behaviours of SPCs is essential to minimize uncertainties as much as possible. Several European projects from the wind industry, such as WIND EUROPE [24], CARBON TRUST [25,26], and ETIPWind [7], are advocating for studies on SPCs. Notably, CARBON TRUST [25,26] and ETIPWind [7] have emphasized the need for design tools specifically developed for the local mechanical analysis of SPCs, to demystify the complexities for cable engineers.

To respond the callings, recent years have seen the development of guidelines and standards for SPCs. Notably, DNV, IEC, and CIGRE [27–30] have emerged as leading authorities in establishing SPC standards. Three methods can be used to perform the local mechanical analysis of SPCs in practice: analytical, numerical and experimental method [31]. These three methods have their own pros and cons, and usually supplement each other during the design process. Currently, the research on the topic is still quite scarce. There is a clear need to review the existing research on this topic, exposing the challenges so that cable engineers gain the state-of-the-art development of analysis methods before further actions are taken. For this purpose, this paper provides a comprehensive review of the existing methods for the local mechanical analysis of SPCs. An examination of the experimental (Section 2), analytical (Section 3) and numerical methods (Section 4) are reviewed sequentially. Section 5 synthesizes these discussions, providing guidelines for utilizing these methods, and identifying key challenges that must be addressed in order to develop potential effective methods.

2. Experimental method

Mechanical analysis towards flexible structures have been conducted for a long history [32,33] mainly for the safety consideration as these structures also encounter complicated loadings when they are exposed in the ocean environment [34]. Now that SPCs are

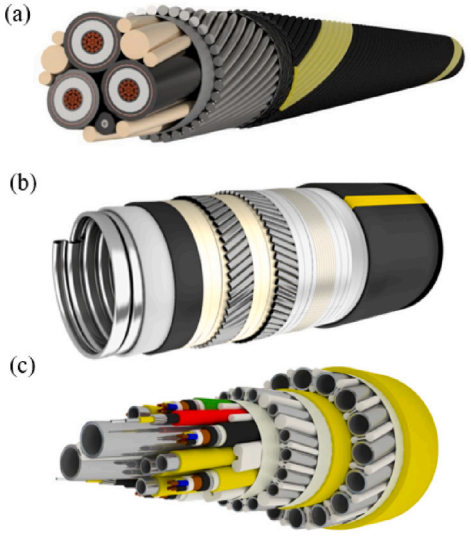

Fig. 5. An SPC (a) [14], a flexible pipe (b) [17] and an umbilical (c) [18].

gradually utilized in harsher environment and there are more fragile components within this particular structure, such as conductors and insulation whose stress variation is crucial [35], yet the analysis and emphasis of SPCs are not exactly the same as those in a traditional flexible structure. Although the configuration of SPCs is also gradually evolving and becoming different from a typical flexible structure such as flexible pipes and umbilicals, there is still much shared useful knowledge. Therefore, the review will cover the previous important research and standards regarding typical flexible structures as well in the experimental, analytical and numerical parts.

The purpose of common tests regarding flexible structures is to observe and obtain the mechanical behaviour of the target structures under the loadings that the structures might encounter in real-life scenarios, including tension, torsion, pressure, bending, compression and any possibilities of their combinations. In addition, the observations and data from tests can guide the research & development of analytical models and numerical models, finally validating their credibility and reliability. For example, as CIGRE [30] points out, measurements of the curvature-moment relationship of an SPC sample can be useful as a tool to calibrate and verify its cross-section model. In these common loadings, tension and bending are two of the most-frequently mentioned loadings in the brochure given by CIGRE [30], therefore, this review will mainly focus on these two loadings and their combination, however, the other loading cases will be covered as well when related.

2.1. Axisymmetric loading tests

API RP 17B [36] lists the procedure for performing tension tests. One end of the sample is fixed, and an axial load is applied to the other end. The load application should be sufficiently slow to avoid dynamic amplification. The maximum loading rate should not exceed 5% of the expected maximum load per minute. As a guideline, the load application should be completed in approximately 5 min. Unless otherwise specified in the details for particular tests, the tests shall be carried out at an ambient temperature of $(20 \pm 15)°C$ [30].

The sketch of a typical tension sample is shown in Fig. 6. The end effects can be reduced as much as possible if the sample length is as long as possible. However, the cost and laboratory conditions should also be considered. In the test recommendation given by the CIGRE guidelines [30], it is required that the length of the test cables be at least five times the pitch length of the outer armour layer. It is required that the minimum length of the test sample, excluding end fittings, i.e., the effective length in Fig. 6, should be two times the pitch length of the outer armour layer [36].A tension test facility is shown in Fig. 7 for a reference. A few examples of flexible structure tests are organized in Table 2 for a reference, where the key information such as the sample length, pitch and loading rate is given if available.

As tension tests regarding SPCs are scarce in the open literature, relevant information is found in four papers [41–44]. Unlike flexible pipes and umbilicals, a power cable is usually preloaded before a tension test starts due to the existence of more gaps caused by the magnitude of helical components within this structure. Helical components induce substantial gaps that need to be eliminated by the preloading process. After this manipulation, the stiffness will not be the same. As an example, after the cables are loaded and unloaded three times, according to the axial tension-axial displacement curves from Nam et al. [41], it is observed that the tension stiffness, i.e., the slope of the curve, is basically linear for the tests. Noteworthy, Nam et al. [41] applied an initial longitudinal displacement of 0.5 mm (a load of approximately 20 kN) on the cable prior to the test to minimize the deflection caused by the self-weight. They found that the stiffness in the first loading is slightly lower, then the stiffness in the next two loading rounds becomes larger and tends to a stable value. This is due to the presence of small gaps between each component layer after the

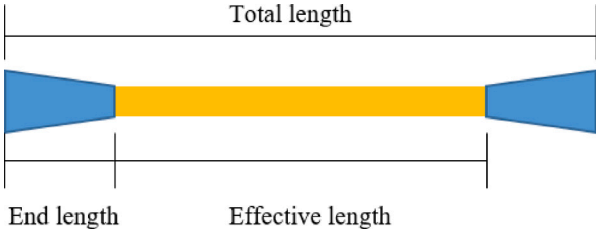

Fig. 6. Sketch of tension test.

Table 2
The available tension tests in the literature.

Structure type	Diameter	Total length	Effective length	Pitch length	Loading rate
Fibre glass reinforced flexible pipes [37]	76	1800	1000	4.26	1 mm/s
Metallic strip flexible pipes [38]	74	1780	1100	57	1 mm/s
Umbilicals [39]	104	3000	–	125	slowly
Umbilicals cable [40]	95.7	2500	–	237	0.5 mm/min, 1 mm/min and 2 mm/min
Three-core SPC [41]	–	6500	–	–	force loading
Three-core SPC [42]	158.2	10 000	–	–	6.5 KN/min
Three-core SPC [43]	–	30 000	–	<30000/5	force loading

The unit is in mm if not written explicitly; '–' means the information is unavailable.

Fig. 7. Tension test facility [41].

fabrication of SPCs [45]. The gap was minimized or removed substantially after the first uniaxial tensile test. Consequently, the axial stiffness measured from the second and third loadings became constant.

Similarly, Guo et al. [42] also conclude that the degrees of stiffness in the later two rounds become larger than the first loading. The authors also observed that the axial stiffness during the unloading period is slightly smaller (about 3%) than during the loading period. Paiva et al. [44] performed a series of tests to validate the stress of the helical wires by inserting sensors into their cable. The cable sample used by Dos Santos Paiva is a three-core SPC with bitumen sticking to the armour layers. The strain gauges were attached through small windows on the outer sheath to measure the variation in the deformation of the helical wires, as shown in Fig. 8. The detailed values from the gauges are extracted and validated against their simulation results.

SPCs also suffer from torsion, which affects their behaviour in actual situations. CIGRE [30] emphasizes that torsion stiffness is a crucial parameter in cable design, as it is in the design of flexible pipes [36]. However, neither standard provides detailed test setup procedures [30,36]. Pure torsion tests on SPCs are quite rare. In fact, as of this review, there is only one documented pure torsion test on SPCs in the open literature. Grant, William et al. [43] obtained torsion stiffness from a tension test, where one end of the sample was completely fixed while a torque was applied to the other end. The torsion stiffness is determined by:

$$GJ = \frac{T}{\tau} \tag{1}$$

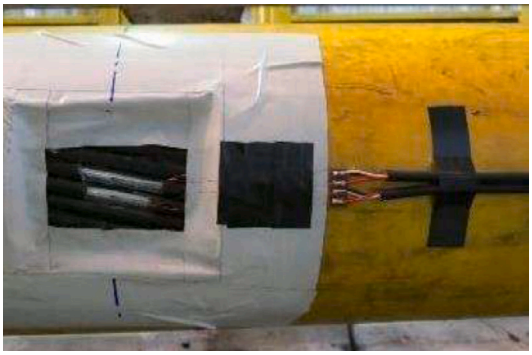

Fig. 8. Strain gauges installation [44].

Table 3
The available torsion tests in the literature.

Structure type	Diameter	Total length	Effective length	Pitch length	Loading rate
Three-core SPC [43]	–	63 000	–	<30000/5	–
Fibre glass reinforced flexible pipes [47]	76	–	1000	4.26	0.18 deg/min
Metallic strip flexible pipes [46]	78	1690	1010	61	6 deg/min
Reinforced thermoplastic pipes [48]	<167	1000	–	–	0.1 deg/s
Umbilicals [49]	93	–	6300	–	–

The unit is in mm if not written explicitly. '–' means the information is not available.

where $GJ(\mathrm{Nm}^2/\mathrm{rad})$ is the torsion stiffness, $T(\mathrm{Nm})$ is the applied torque, and $\tau(\mathrm{rad/m})$ is the torsion angle per unit length. The torque was applied in two opposite directions during their test, revealing different behaviours in the cable. The winding direction of the outermost wires in their cable sample is negative. When a positive torque is applied in the opposite direction, the outermost wires move outward, resulting in slack in the cable. Conversely, when a negative torque is applied, the outermost wires move inward, causing the cable to become tighter. This phenomenon results in different torsion stiffnesses depending on the direction of the applied torque. Specifically, when the applied torque and the winding angle of the outermost wires share the same direction, the cable becomes tighter and the torsion stiffness increases. The authors explain that this observation is mainly due to the variation in contact pressure between the wires and the outermost serving layer. When the two directions are opposite, the wires move outward, decreasing the contact pressure and, consequently, the torque. Conversely, when the directions are the same, the wires move inward, increasing the contact pressure and the torque.

Torsion tests on other flexible structures are also reviewed for the convenience of the readers, and their details are provided in Table 3. The phenomenon of different torsion behaviours under opposite torsion directions observed in [43] is also noted in [46], where an unbonded metallic strip flexible pipe was tested under torsion. A significant stick–slip issue was found in this structure, which could also be an important concern in SPCs, where the components are similarly unbonded.

Another type of axisymmetric loading is compression. This loading has not been included in some cable standards such as IEC [50], which CATAPULT [51] has highlighted as a serious issue. A DPC is likely to be subjected to axial compression, i.e., negative tension, due to the dynamic motion of the cable and/or platform. Compression on the armour wires creates an outward radial force that could potentially lead to the failure of the outer sheath, a phenomenon known as birdcaging. If the outer covering is sufficiently strong, negative tension could instead cause local buckling [30]. It has also been found that compression, in combination with cyclic bending of SPCs, can trigger lateral buckling of the armour wires.

The test procedure is clearly outlined in CIGRE [30], as well as in a paper by Karlsen et al. [52]. However, the reviewers found the details provided by Reda et al. [53] to be more elaborate, including the facility arrangement and the analysis of their test results. Considering the limited number of research papers on the topic of compression, this paper is a valuable starting point. Reda et al. performed both compression tests and combined compression and bending tests. The corresponding facility arrangements are shown in Fig. 9(a) and Fig. 9(b), respectively. Notably, for the combined compression and bending test, a high-strength steel wire rope was installed through the cable in the axial direction. The steel wire rope was fixed to one end of the cable and was used to apply the compressive force onto the cable during the test. The authors found from their test results that the axial stiffness under compression was 32 times lower than the axial stiffness under tension.

2.2. Bending tests

Several test methods can be used to measure the bending stiffness of an SPC. CIGRE TB 669 [30] and Coser et al. [54] described three common test principles on which bending tests on SPCs are based: the three-point bending method (also termed single-point

Fig. 9. Test arrangement of compression (a) and combined compression and bending (b) [53].

load method), four-point bending method (termed two-point load method) or moment method. The first two are more common in the open literature. For the three-point bending, a concentrated force is applied to the middle of a structure, which might cause structural collapse. This test facility is more recommended to obtain the critical bending loading, though it can also be used to predict bending stiffness. The four-point bending test facility, instead, prevents abrupt structural collapse as much as possible.

A classical four-point bending test sketch is given by CIGRE [30], as shown in Fig. 10. A cable is supported by two rotating fixtures, enabling axial sliding with minimal friction. This capability is facilitated by either rollers or supports crafted from materials with low-friction properties. Consequently, a uniform bending moment, devoid of shear force, can be attained between the two inner supports. The test normally generates a curvature-bending moment curve that needs to be calculated based on the configuration of test setups. The resulting moment M over the cable between the inner supports is given by:

$$M = \frac{FL_2}{2} \tag{2}$$

where F is the applied force and L_2 is the distance between the inner and outer supports. The curvature can be estimated from the displacement of the cable and the two supports that are connected to the moving frame by:

$$\kappa = \frac{8(S_1 - \frac{S_2}{2} - \frac{S_3}{2})}{L_1^2 + 4(S_1 - \frac{S_2}{2} - \frac{S_3}{2})^2} \tag{3}$$

where κ is the cable curvature, S_1 is the displacement of the centre of the sample relative to a straight position, S_2&S_3 are the displacements of the two supports relative to when the sample is in a straight position, and L_1 is the distance between the two inner supports. Should a dynamic bending stiffness be measured, the loading supports should be specially designed to satisfy the cyclic bending in two opposite directions. A typical dedicated test-rig for a full-scale four-point bend test can be found in, for example, Tyberg et al. [55], as shown in 11.

The length is crucial in preparing bending samples as it affects the predicted stiffness significantly. Although sample lengths are recommended to have at least one pitch length of the outer armour layer [30], actual physical lengths chosen by experimenters are usually much longer [56]. Table 4 shows detailed information on bending tests done by scholars. Unlike those in the tension test, the influences from temperature and loading rate have been more tested by the experimenters. Whether or not the influence from these two factors is tested is summarized in Table 4. Tests are usually performed in a cyclic manner to measure bending stiffnesses until a stable hysteretic response is achieved. This results in a hysteretic curvature-bending moment curve, as Fig. 12.

When the curvature is low, friction among the components is sufficient to resist slippage, resulting in a relatively higher stiffness, i.e., the slope of the curve. Stiffness in this scenario is called stick stiffness. However, as the curvature increases, a point is reached where the friction is not enough to prevent the components from slipping, slowing down the increased speed of the bending moment and reaching the slip stiffness. These phenomena can be observed from Fig. 12. Slip stiffness can be several orders of magnitude lower than stick stiffness [30]. When the bending direction is reversed, friction needs to be overcome in the opposite direction, resulting in a hysteretic curvature-moment relationship. In this example, the cable is first bent to a positive curvature, then to a negative curvature, and then back to a positive curvature again, creating a hysteresis loop. This type of curvature is observed by bending tests on cables [43,55–57], as well as on copper conductors [59,60], flexible pipes [61–64] and umbilicals [49,65].

As the temperature variation during the service scenarios ranges substantially and there is polymer material whose material property is strongly affected by the temperature variation, CIGRE [30] and IEC [29] recommend the bending test should also

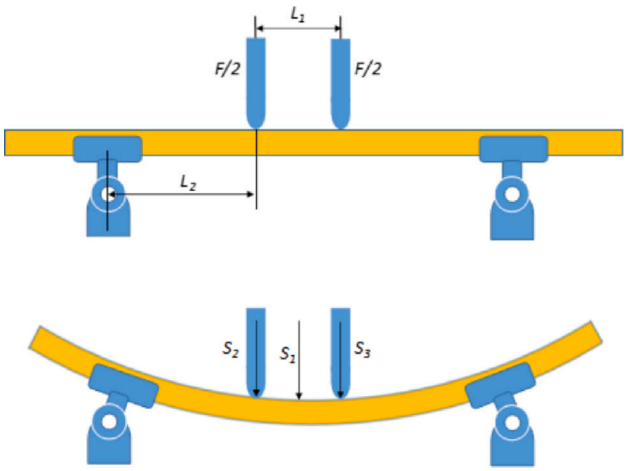

Fig. 10. Illustration of test setup utilizing four-point bend method [30].

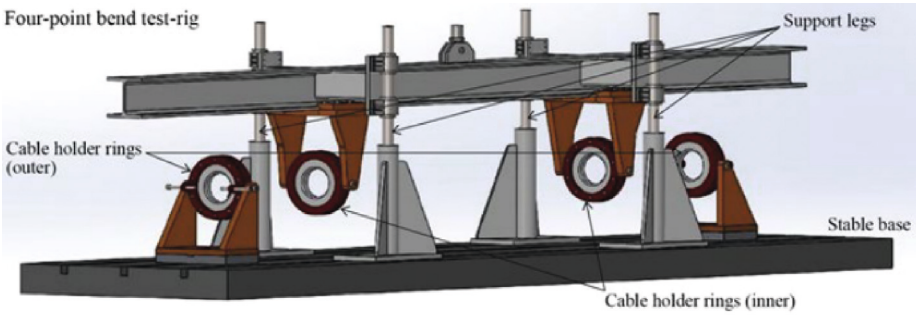

Fig. 11. Dedicated test-rig for full-scale four-point bend test [55].

Table 4
The reviewed bending tests in the literature.

Author	Test method	L/D	L/Pitch	Thermal	Loading rate
Maioli [57]	Three-point bending	>20	–	Yes	Yes
Tyberg et al. [55]	Four-point bending	–	–	Yes	No
Komperød et al. [58]	Four-point bending	–	–	Yes	Yes
Fabien et al. [56]	Four-point bending	25	3.42	No	No
Coser et al. [54]	Cantilever beam and three-point bending	17.77 and 46.6	–	No	No
Delizisis et al. [43]	Three-point bending	–	–	No	No

'–' means the information is unavailable.

be performed under different temperature to obtain the corresponding bending stiffness. Maioli et al. [57], Tyrberg et al. [55], Komperød and Magnus [58] took the thermal effect into account in their tests, and it is found that the thermal effect is indeed a significant factor in determining the bending stiffness. The curvature-moment curves obtained by Komperød and Magnus [58] are shown in Fig. 13 for an example. The test was performed at two different temperatures and two different loading rates. When the ambient temperature changes from $5°C$ to $20°C$, the moment becomes twice smaller. This might cause the notorious overbending failure [27] if not considered properly. The influence of loading rate can also be observed from Fig. 13.

It is commonly known from the flexible pipe industry that stiffness can be affected by combined loadings. For example, tension significantly affects the bending stiffness [66]; So does external pressure on bending and torsion stiffnesses. Plus, they are all very common combination styles that a cable suffers from in real life. However, these combination loading tests require specially designed test facilities, which are not easily attainable [67]. There is only one paper presented by Coser et al. [54] that introduces the setup of the facility for SPCs under combined loadings. The test results show that the bending stiffness is significantly affected by tension forces. The setup of their test facility is shown in Fig. 14. The test rig had two hydraulic actuators, an axial actuator and a transversal actuator. The former generates a tension force, while the latter bends the test sample. With this test setup, it was possible to obtain the bending stiffness of the cable under different axial tensions.

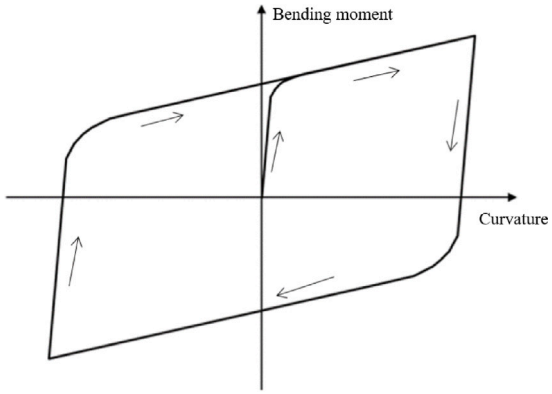

Fig. 12. Hysteretic curvature-bending moment curve [30].

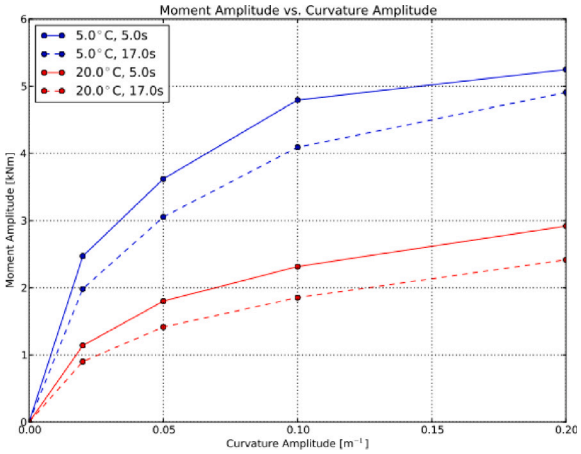

Fig. 13. Curvature-bending moment curve under different temperature and loading speed [58].

2.3. Remarks on experimental method

While testing is considered fundamental and reliable, it comes with several limitations:

1. Each SPC is project-based. Its structural configuration differs from case to case. Tests need to be done specifically for a target SPC, thus they are costly and time-consuming. Besides, in the preliminary design phase, a cable sample is not available, making it hard to conduct tests.

2. The measurement of the local mechanical behaviour of the inner components in SPCs is scarce in the open literature, as SPCs are complicated multi-layer structures. Test methods are hard to provide insights into their internal mechanisms and how they propagate within structures; thus, internal behaviour is like a black box to engineers [31,51,68,69].

3. SPCs in real-world applications are subject to combined loadings, such as tension coupled with bending. Setting up facilities to replicate these complex conditions is exceedingly difficult [54].

However, tests are still necessary throughout the life cycle of an SPC. The test data can be used to guide the development of analytical or numerical methods, and serves as a validation tool for the developed model. Besides, relevant test data is needed to calibrate the missing value of an SPC sample. CIGRE [30], for example, states that measurements of the curvature-moment relationship can be useful as a tool to calibrate the equivalent pressure induced by the initial residual stress. As this dissertation aims to develop an effective modelling method for the local mechanical analysis of SPCs, the proposed method needs to be validated by test data, and the previous research on experimental methods is reviewed. Two major points need to be paid attention to when performing corresponding test:

• The sample length is a crucial parameter in affecting the overall mechanical behaviours of SPCs. A proper length is relevant to the sample diameter and the pitch length of the inner components. In a tension test, the sample length should be at least five times the pitch length of the outer armour layer. For the bending case, the recommended length given by standards is at least longer than one pitch length of the outer armour layer; however, the sample lengths selected by experimenters are usually longer.

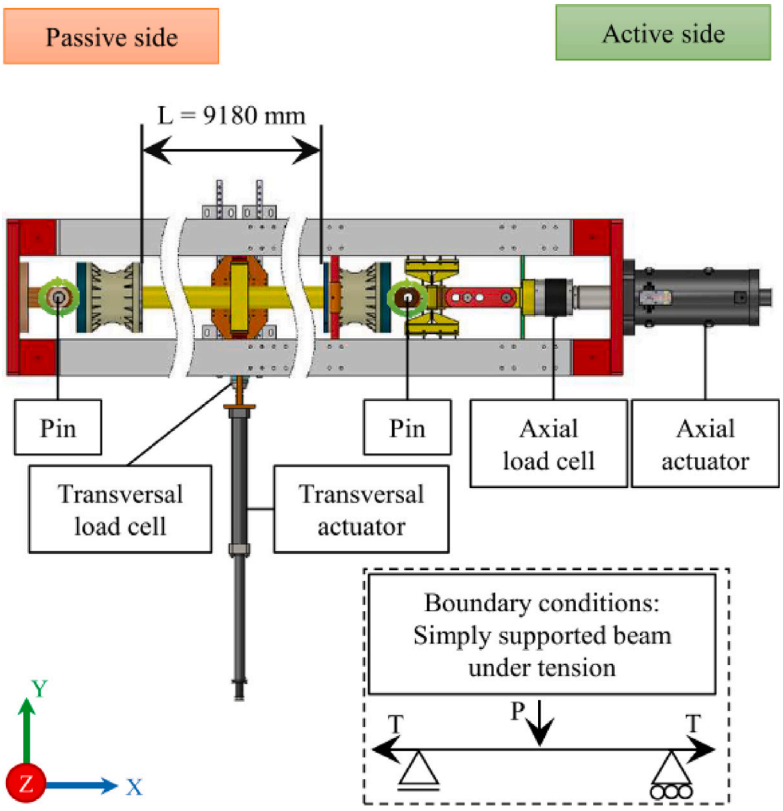

Fig. 14. Setup for combined tension and bending test [54].

• The loading rate and temperature have been found to be crucial factors affecting the overall mechanical behaviour of SPCs. The loading process should be sufficiently slow to avoid dynamic amplification, and normally the test should be carried out under room temperature.

3. Analytical method

This section explores the analytical methods used to perform local mechanical analyses on flexible structures, focusing on SPCs. In the analysis of SPCs, tension, torsion, and external pressure are often grouped together as axisymmetric loadings. To facilitate understanding, the discussion is divided into subsections dealing with axisymmetric loadings and bending separately.

Before diving into specific methodologies, it is important to establish the common assumptions applied in the analytical study of SPCs:

a. Strain Consistency: The strain is assumed to be constant along the length of the structure.

b. Small Deformations: Only small deformations are considered, aligning with the linear elastic framework.

c. Helical Wire Spacing: Helical wires in any layer are assumed to be equally spaced around the cable's circumference, simplifying the analysis by ignoring the contact between wires in the same layer.

d. Simplification of Components: Copper conductors and steel strands are modelled as solid cylinders, which simplifies complex real-world geometries into more manageable forms for mathematical analysis.

These assumptions are crucial for applying analytical methods effectively and are supported by Refs. [41,43,70,71]. They set the foundational conditions under which the subsequent analyses are conducted, ensuring that the complexities of SPC behaviours are addressed within manageable and realistic constraints.

By setting these premises, the section prepares to delve into the detailed mechanical behaviours of SPCs under specified loading conditions, providing a framework that supports robust and precise mechanical predictions.

3.1. Axisymmetric loadings

The tension stiffness in analytical methods is derived based on the principle of superposition, where the contributions from all components are cumulatively added. According to this principle, the equation for tension stiffness is expressed as follows:

$$K = A_c E_c + K_w \tag{4}$$

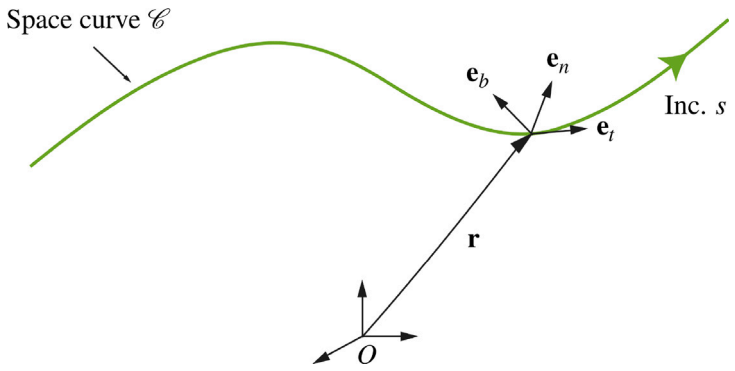

Fig. 15. Kirchhoff rod illustration [76].

Table 5
The information of available analytical studies on SPCs under axisymmetric loadings.

Author	Cable types	Wire DOFs	Contact	Thickness variation
Grant et al. [43]	Three-core SPC	u1	No	No
Chang et al. [70]	Three-core SPC	u1, u3, u6	No	No
Nam et al. [41]	Three-core SPC	u1, u3, u4, u6	Normal contact	Yes

In this equation, the subscript c denotes cylinders and w denotes wires, which include helical wires and other helical components. Here, A_c represents the cross-sectional area, and E_c is the Young's modulus of the cylinders. Helical components, being structurally complex, have been the focus of several studies [41,43,70] due to their unique mechanical behaviours. Given that their cross-sectional area is significantly smaller than their length, helical wires are typically modelled as thin curved rods in analytical assessments. The complexities introduced by the helical configuration have garnered considerable research interest, highlighting the need for meticulous analysis to understand their influence on overall cable behaviour.

The foundational theory of thin curved rods can be attributed to Kirchhoff, who developed the linear theory of slender curved rods in the mid-19th century [72]. This seminal work is further explored in Love's comprehensive treatise [73] and elaborated upon by Ericksen and Truesdell [74]. Kirchhoff's theory posits that an elastic rod's centreline is inextensible and that its cross-sections remain plane and normal to the centreline throughout deformation [75].

An illustration of a Kirchhoff rod, depicted in Fig. 15, demonstrates the rod's three translational degrees of freedom (DOFs) and three rotational DOFs. The unit vectors $\boldsymbol{e}_t$, $\boldsymbol{e}_n$ and $\boldsymbol{e}_b$ represent the directions tangent, normal, and binormal to the curve, respectively. The vector $\boldsymbol{r}$ denotes the position of the target point of the wire relative to the origin of the Cartesian coordinate system.

Under Kirchhoff's theory, several critical assumptions are made to simplify the analysis:

a. Cross-sections of the rod remain planar and perpendicular to the neutral axis during any deformation.

b. Strain within the rod is minimal, allowing the material to maintain its linear elastic properties throughout deformation.

c. Shear deformation effects are considered negligible, focusing analysis purely on bending and twisting responses.

Kirchhoff's theory is particularly applicable when the rod's length significantly exceeds its diameter, a condition referred to as a high slenderness ratio, and when deformations remain minimal. A comprehensive theoretical exploration of Kirchhoff's rod theory is provided by EH Dill [77]. Due to its generality, this theory has been extensively applied across diverse research fields that involve helical structures, as evidenced by its application in studies by Schlick et al. [78], Goyal et al. [79,80], Yang [81], and Wang [82].

Focusing on the behaviour of single wires, Dong et al. [83,84] conducted detailed analyses of the curvature variations of a single helical wire interacting with a neighbouring cylinder. These studies are crucial for understanding the local mechanical dynamics within layered helical systems.

Additionally, Knapp [85] developed a stiffness matrix for helically armoured cables using the energy method, addressing the interaction between tension and torsion. His findings reveal that axial tension in cables can induce torsional forces, although his model simplifies the analysis by omitting the curvature variations of helical wires in their three local directions.

Despite the breadth of research in flexible structures, analytical models tailored specifically for SPCs are notably rare. To date, only a few studies, including those by Chang et al. [70], Nam et al. [41], and Delizisis et al. [43], have provided analytical formulas for SPCs under axisymmetric loadings. The methodologies from these studies are detailed in Table 5, highlighting the translational and rotational degrees of freedom (DOFs 1–6) that correspond to the vectors e_t, e_n and e_b illustrated in Fig. 15.

Grant et al. [43] obtained the stiffness contributed by the helical wires by superposing the contributions from all the wires, using the formula in Eq. (5), where the subscript j means the layer number, n is the number of wires in the corresponding layer, E is Young's modulus, A is the wire cross section and α is the winding angle. These parameters are illustrated in Fig. 16. Only the deformation in the u1 direction is considered in this formula. Grant et al. also gives the torsion stiffness K_4 [43], shown in Eq. (6). In this case, the wire stress σ_j is the product of Young's modulus E, the axial strain of the cable δ and $\cos^2\alpha_j$, given in Eq. (7).

$$K_1 = n_j E_j A \cos^3\alpha_j \tag{5}$$

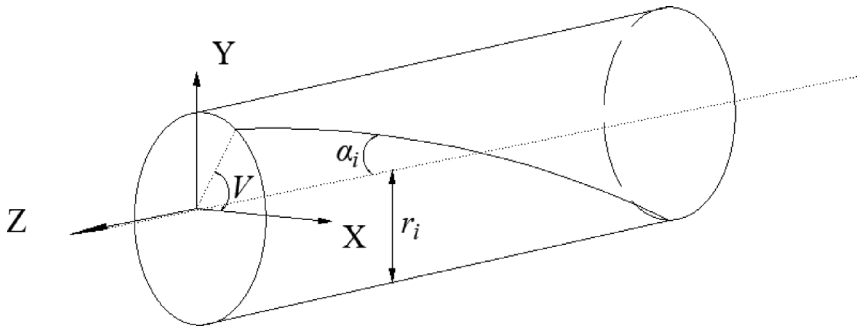

Fig. 16. Helical wire on a cylinder.

$$K_4 = n_j E_j A r_i^2 \cos\alpha_j \sin^2\alpha_j \tag{6}$$

$$\sigma_j = E\delta\cos^2\alpha_j \tag{7}$$

Chang et al. [70] further consider the deformation of helical wire in u3 and u6 directions based on Knapp's derivation [85]. Assuming no torsion coupled, the axial stiffness thus becomes:

$$K_1 = n_j E_j A(\cos^3\alpha_j - \frac{u_R}{r_j\delta}\sin^2\alpha_j \cos\alpha_j) \tag{8}$$

The physical meaning of the new-added term $-n_j E_j A\frac{u_R}{r_j\delta}\sin^2\alpha_j \cos\alpha_j$ is the effect from radial strain on the axial stiffness, where u_R is radial displacement in the cable radial direction. The torsion stiffness given by Chang et al. [70] is the same as that given by Grant [43] in Eq. (6). In this case, the wire stress is given by the following equation, where θ is the rotation angle of the cable in unit length.

$$\sigma_j = E(\delta\cos^2\alpha_j - \frac{u_R}{r_j}\sin^2\alpha_j + r_j\theta\sin\alpha_j\cos\alpha_j) \tag{9}$$

Nam, Woongshik et al. [41] developed analytical methods that account for the curvature changes of helical wires and variations in the thickness of all layers. Their approach, rooted in the principle of minimum virtual work, is compiled into a matrix framework for analysis [86]. However, due to the complexity and number of deformations considered, their model often requires supplementation with numerical methods for direct solution.

Despite these advances, current models [41,43,70] generally overlook the specific contributions of inner helical components to the overall mechanical properties of the cable. This oversight is significant as the helical shape of these inner components can profoundly influence cable tension behaviours. Historically, these inner helical components are assumed to be straight during tension analyses [87], a simplification that may not accurately reflect their actual mechanical contributions.

3.2. Bending

Analytical methods tailored specifically for SPCs are notably lacking, particularly concerning bending scenarios. Existing models from related fields, such as flexible pipes or umbilicals, cannot be directly applied to SPCs for several reasons. Flexible pipes are designed with a hollow cross-section to facilitate the transportation of oil and gas. Similarly, umbilicals do contain central components; however, these are typically made from non-metal materials with a relatively low Young's modulus. In both cases, the structural integrity is primarily provided by the outer metal layers, such as armour layers.

In contrast, SPCs incorporate metal components within their core, significantly influencing their structural properties. These central metal components are often helical and involve intense contact interactions, adding complexity to their mechanical behaviour.

One of the critical issues in the bending analysis of SPCs is the stick–slip phenomenon, which is influenced by contact pressure and the friction coefficient. These factors are intrinsic properties of an SPC and should be provided by cable manufacturers. The contact itself is often a result of radial initial pressure combined with residual stresses in the polyethylene (PE) sheath from the extrusion process. Currently, there are four main approaches to model the effects of these factors: using equivalent external pressure, equivalent internal pressure, tension force, or stresses induced by thermal variations in the polymer materials [88–90]. These methods will be explored further in Section 4.

Furthermore, the determination of when and how wires begin to slip during bending is governed by the contact pressure and friction coefficient. There are two classical assumptions about the path of slip in the literature, visualized in Fig. 17:

Table 6
The slip path assumptions in analytical studies.

Slip path assumptions	Papers
Geodesic	Feret & Bournazel, 1987 [91] Feret & Momplot, 1991 [92]
Loxodromic	Berge, et al. 1992 [93] Sævik, 1992 [94] Kebadze & Kraincanic, 2000 [95] Sævik, 1993 [96] Lukassen, 2019 [97]
Others	Estrier, 1992 [98] TAN, et al. 2005 [99] Fergestad & Løtveit, 2014 [100]

Geodesic Path: This path is defined as the shortest path between the intrados and extrados on the neighbouring cylinder, as depicted in Fig. 18. Under this assumption, a transverse slip occurs without any curvature change in this direction.

Loxodromic Path: This assumes that the wire maintains its position relative to its neighbouring layers during bending, potentially causing curvature variations in this direction.

The debate between adopting a geodesic or loxodromic path underlies many studies in the analysis of flexible pipes under bending. The actual response of a structure is likely to lie between these two theoretical paths, as detailed in Table 6.

Existing research found that the assumption of the loxodromic path is closer to reality after comparison with test results and thus is used more frequently in studies [93–97]. Based on the assumption of the loxodromic path and the Kirchhoff rod theory, the stress on the wire before it starts to slip can be given as:

$$\sigma_i^{stick} = E_i \cdot \kappa \cdot r_i \cdot \sin V \cdot \cos^2 \alpha_i \tag{10}$$

where κ is the cable curvature. As long as the friction stress along the wire is greater than σ_i^{stick}, the wire will continue to adhere to its neighbouring layers. Otherwise, the wire starts to slip. The friction force exists only when there is inner normal stress caused by, for example, residual stress, an external pressure or the normal contact stress component resulted by a tension force. Feret gives the pressure differential contributed by tension through each layer [91], as shown below:

$$\Delta P_j = \frac{n_j \sigma_j A_j \sin \alpha_j \tan \alpha_j}{2\pi r_j^2} \tag{11}$$

Therefrom, the contact pressure P between two neighbouring layers after considering an external pressure P_{ext} becomes:

$$P_j = \Delta P_j + P_{ext} \tag{12}$$

As there are gaps among wires in armour layers, the pressure needs to be distributed to each wire using a fill factor F_f. Sævik [101] defined this value for rectangular wires used in flexible pipes as:

$$F_{f,j} = \frac{n_j b_j}{2\pi r_j \cos \alpha_j} \tag{13}$$

where b is the width of wires with rectangular cross-sections. Nevertheless, the wires used in SPCs are mainly made into round cross-sections where the fill factor needs to be adjusted. Assuming the fill factor is satisfied for round helical wires, the contact pressure on each wire is given by:

$$P_j = \frac{P_j}{F_{f,j}} \tag{14}$$

Once the contact pressure is known, the friction force can be derived as:

$$f = \mu P_j \tag{15}$$

Therefore, as long as $f = \sigma_i^{stick}$, slip starts to appear. Wires on a region of a cross-section slip while wires on the other region still stick, as shown in Fig. 19. The limit curvature is thus obtained:

$$\kappa_{\lim it} = \frac{\mu P_j}{Et \cos V \cos^2 \alpha_j \sin \alpha_j} \tag{16}$$

where t is the thickness of wires with rectangular cross-sections. It can be derived from Eq. (16) that the slip first appears at the angular position $V = 0; V = \pi$. After the applied curvature surpasses $\kappa_{\lim it}$, the slip area will enlarge and gradually progress, then there will be a slip area and a stick area, as shown in Fig. 19. The transition angle V^* between these two areas can be obtained:

$$V^* = \arccos\left(\frac{\mu P_j}{Et \cos^2 \alpha_j \sin \alpha_j k}\right) \tag{17}$$

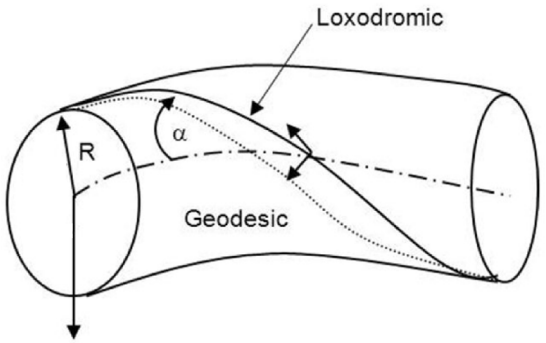

Fig. 17. Geodesic and Loxodromic curves [103].

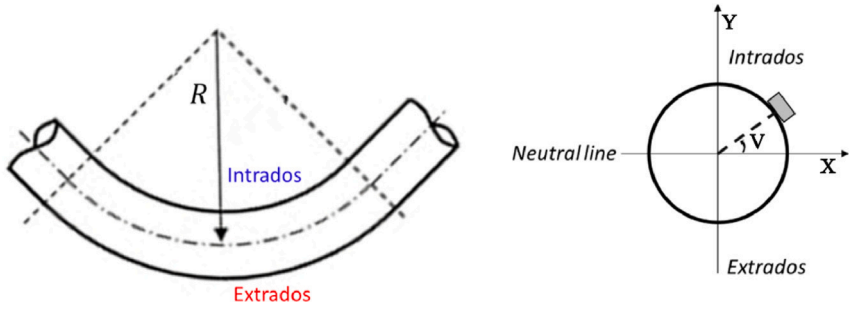

Fig. 18. Illustration of the intrados and extrados [103].

In the slip area, the wire stress is:

$$\sigma_i^{slip} = \frac{\mu P_j r_j}{t \sin\alpha} V \tag{18}$$

The axial slip displacement is also mentioned in the literature [91,102] by a simplified equation as:

$$u_{slip} = r_j{}^2 \frac{\cos^2\alpha_j}{\sin\alpha_j} \kappa \cos V \tag{19}$$

Finally, the bending moment contributed by all the helical wires can be integrated over the cable cross-section as:

$$M_w = 4\left(\int_0^{V*} \sigma_{slip} A_j dV + \int_{V*}^{\pi/2} \sigma_{stick} A_j dV\right) \tag{20}$$

3.3. Remarks on analytical method

To date, only a limited number of studies, such as the one by Tjahjanto et al. [71], have attempted to provide an analytical method for evaluating the stress in an SPC, particularly addressing the effects of helical components. Although these components, including inner helical conductors, are crucial in influencing component stresses, the study does not comprehensively address the overall behaviour of the SPC. Additionally, the method for managing pressure across each layer remains unspecified, highlighting a gap in the analytical approach.

In summary, while analytical methods offer a framework to predict the overall mechanical behaviour of SPCs, several challenges emerge, particularly at the component level:

1. Complex Contact Pressure: Analytical methods struggle to accurately capture the complex contact pressures among layers, which are critical in determining the local mechanical behaviour of SPCs under bending. This is largely due to the dense arrangement of helical components within the cable.

2. Simplification of Helical Wires: Previous studies often simplify the helical wires in the armour layers as Kirchhoff rods and make specific assumptions about their slip paths. However, inner helical components, which differ from slender beam-like structures, are not adequately studied, and analytical insights into these components are lacking.

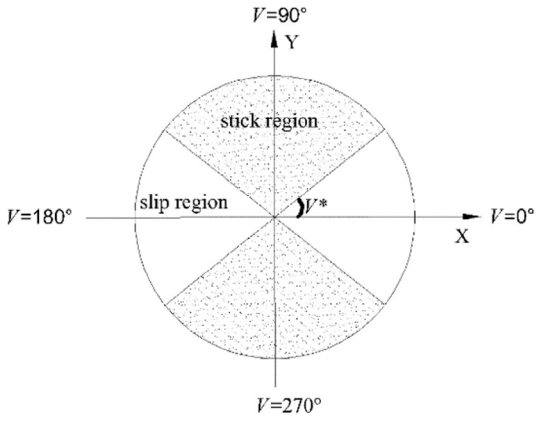

Fig. 19. Stick and slip zones on a cross section.

3. Limitations of Closed-form Solutions: When the model incorporates many detailed features, deriving simple closed-form solutions becomes impractical. Consequently, such complex models require numerical solutions to resolve [104], pushing the boundaries of traditional analytical methods.

4. Numerical method

When considering the intricate details necessary for accurately modelling SPCs, a large number of partial differential equations (PDEs) emerge, necessitating numerical solutions. Common numerical methods employed include the finite difference method, finite volume method, boundary element method, and notably, the finite element method (FEM). FEM is particularly adept at addressing problems characterized by complex geometries, diverse material properties, intricate contact interactions, and multi-physical problems, making it the preferred choice for solving PDEs in this domain. Enhanced computational capabilities of modern computers have facilitated efficient PDE solutions via FEM, allowing designers to visually explore mechanical behaviours at both the overall and component levels of SPCs.

Despite the strong capabilities of modern computers and algorithms, an SPC is too complex to be fully calculated if all details are included in an FEM model. Therefore, some components need to be simplified, and certain influencing factors ignored for computational efficiency when analysing the overall cable. For instance, common simplifications in studying the overall SPC include modelling the inner copper conductors as solid components and ignoring the effects of thermal or electrical fields [56,71,105–107]. However, in reality, conductors are composed of numerous helical wires (as shown in Fig. 20) and are exposed to varying temperatures due to current. Regarding the insulation layer, it might experience water treeing or electrical treeing in practice if the electrical field is coupled with the mechanical field [20]. Accounting for all these details is highly complex, so researchers often isolate specific components from the overall cable for further analysis, with a particular focus on insulation layers and copper conductors.

Fouad and Monssef [108], for example, study the plasticity evolution and predict the damage of conductors by modelling all the helical wires and considering the contact issues within their interfaces. Nasution et al. and Jiang et al. [21,22,109,110] also examine the fatigue behaviour of helical conductors with more complex configurations, validating their numerical models with test data. In recent years, more investigations [111–114] into insulation layers have appeared in the public literature, aiming to understand how electrical and thermal fields affect the insulation layer. The recently published representative papers on these topics are reviewed and summarized in Table 7 for reference. Notably, these investigations focus on isolated components rather than integrating them back into the overall SPC to observe their behaviour within the original SPC sample.

Compared to studies on single components, numerical investigations on the responses of overall SPCs have attracted significant attention. As mentioned, when studying the overall cable, the inner conductors are typically simplified into solid structures, and the effects of electrical and thermal fields are ignored. These simplifications are consistent with the approaches discussed in Section 3. Both 2D [115,116] and 3D models [70,96] have been developed to analyse flexible structures. However, the greater detail and superior contact simulation abilities of 3D models have driven their increasing adoption in practical engineering. A notable challenge in these simulations is the modelling of numerous helical wires. Researchers have simplified these wires in armour layers of flexible pipes into equivalent tubular layers (orthotropic layer materials) [103,117,118], a process underpinned by equating the axial and bending stiffness of these simplified materials with those of actual layers, drawing on theories from Timoshenko et al. [119].

However, helical wires in SPCs typically differ significantly from those in flexible pipes; they are round with more gaps between them, as opposed to the closely arranged rectangular wires found in flexible pipes, as depicted in Fig. 5(b). This structural difference raises concerns about the accuracy of stress predictions when using simplifications designed for flexible pipes, potentially leading to incorrect stress estimations. Furthermore, such simplifications are less useful when detailed stress analysis of each helical wire is required, thus they have not been widely implemented even in flexible pipe studies.

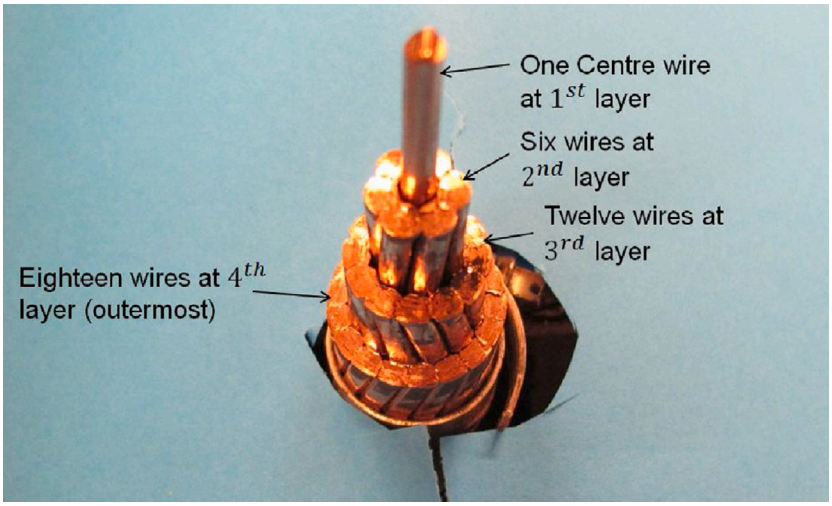

Fig. 20. A photo showing the cross section of a typical copper power conductor [23].

Table 7
Studies on conductors and insulation.

Author and studied components	Plasticity	Thermal	Electrical	Fatigue	Damage
Ech-Cheikh and Drissi-Habti [108] Conductor	✓	×	×	✓	✓
Nasution et al. [21,22,109] Conductor	×	×	×	✓	✓
Jiang et al. [110] Conductor	×	×	×	✓	✓
Miceli et al. [111] Insulation	×	✓	✓	×	✓
Ringsberg et al. [114] Insulation & Conductor	✓	✓	✓	✓	✓

Table 8
The numerical models of SPCs under axisymmetric loadings.

Author	Chang et al. [70]	Hsieh et al. [120]	Fang et al. [86]	Fang et al. [106]
Cable types	Three-core SPC	Three-core SPC	Single-core SPC	Three-core cable
Pitch length	552.4 mm	–	–	–
Model length	941 mm	971 mm	1000 mm	792 mm
Element types	Solid	Solid	Solid + beam	Solid + beam + shell
Interaction	Normal direction	Normal direction	Normal direction	Normal + tangent directions
Algorithms	Static analysis	Static analysis	Dynamic analysis	–

'–' means the information is unavailable.

Constructing each helical wire individually in a detailed 3D model introduces considerable complexity. This approach requires careful selection of element types, meticulous setup of boundary conditions, and precise management of contact properties among interfaces, posing significant challenges in model construction.

4.1. Axisymmetric loadings

Numerical models that address axisymmetric loadings in SPCs are relatively rare in the open literature, with only a few studies addressing this specific challenge. Information on these models is summarized in Table 8.

Full-scale models built in a traditional way are the main focus in [70,86,120] in Table 8. Chang et al. [70] built a 3D model to study the mechanical behaviour of an SPC under coupled tension, torsion and compressive loads. Solid elements are used to simulate all the components within the cable, including the helical wires. Both ends of the cross sections in this model are set as rigid planes with all the nodes coupled to the middle node in the corresponding plane. One end is fully constrained while the loads are applied on the other end.

The interaction normally involves normal contact and tangential contact properties. The former, also known as normal or perpendicular penetration, refers to the interaction between surfaces along their normal direction. The latter, also known as

Table 9
The reviewed numerical study of SPCs under bending.

Author	Tyrberg et al. [71]	Leroy et al. [107]	Menard et al. [56]	Fang et al. [105]
Cable types	Three-core SPC	Three-core SPC	Three-core SPC	Single-core SPC
Pitch length	–	–	383 mm	400 mm
Model length	1/3 core pitch	decided by wire	234.2 mm	20 mm
Element types	Solid	Solid	Solid & beam & surface	Solid
Interaction	Normal + Tangential	Normal + Tangential	Normal + Tangential	Normal + Tangential
Algorithms	–	–	Dynamic analysis	Dynamic analysis

'–' means the information is unavailable.

shear or frictional contact, involves forces exchanged in the tangential direction along the contact surfaces. The most basic method of introducing contacts is to add springs between two contact interfaces. Sævik [96], for example, introduces hyperelastic and elastoplastic springs in the normal and transverse directions to simulate contact in flexible pipes. This is similar to the penalty method used in general FEM software. This method introduces a penalty term into the formulation to enforce contact conditions or constraints when bodies interact. The penalty term acts as a stiffness term that increases as the contact conditions are violated [121,122].

Only the contact in the normal direction is considered in Chang's model [70], where the pure penalty method is utilized. The contact between the cable layers is set to "no separation" for surface contact. Adjacent layers can slide horizontally but not vertically. To avoid the dynamic effect from the loading process, static analysis is selected for the simulation, where the effect from the time item in the dynamic algorithm is eliminated.

There is still no recommendation about how long a 3D model should be to eliminate boundary effects. The model length in [70] is 941 mm, nearly twice the pitch length of the outermost helical wire layer, according to the data provided by the authors. The authors tested the influence of the model length on its tension stiffness, and it was found that the model length stops affecting the tension stiffness significantly even when it is near the pitch length of the outermost helical wire layer. Nevertheless, one thing that should be noticed about this model is that the helical shapes of the inner components are disregarded. The other paper studying SPCs under tension is authored by Hsieh et al. [120], who further investigated the influence of the number of cores on the mechanical properties of SPCs under axisymmetric loadings based on the work of Chang et al. [70]. The details of the model are similar to Chang et al. [70], and the helical inner cores are simplified into straight cylinders again. In addition, Fang et al. [86] also performed the local analysis of single-core SPCs under tension. In this case, the inner components are all straight, thus there is no such simplification that the helical shapes of the inner components are eliminated. In these three papers, the effect of the helical shapes of inner helical components is not accounted [70,86,120].

Very recently, Fang et al. [106] managed to take this factor into consideration by developing an effective modelling method for the local mechanical analysis of three-core SPCs under tension. In this paper, the helical shapes of the inner components are accounted for the first time regarding the tension case in the open literature. The helical shapes have been found to play a not-to-be-ignored effect on the stress of the components within SPCs. For example, Fang et al. [106] found that the contact pressure distribution of the layer that surrounds the inner helical components is uneven, which cause an unexpected stress of the helical wires. The model is shorten significantly after periodical boundary conditions derived by homogenization method on beam-like structures are applied. As this model is based on a repeated unit cell (RUC), it is therefore termed as RUC model. In addition, the authors also built a full-scale numerical model that uses traditional boundary conditions in the models mentioned above [70,86,120]. It is found that the RUC model agrees better with tension test results than the full-scale model, and the RUC model presents higher efficiency as well.

4.2. Bending

Four seminal papers provide detailed 3D numerical models for SPCs specifically under bending conditions, with their findings summarized in Table 9. Each of these models, developed for three-core SPCs and single-core SPCs, varies in terms of how inner helical shapes are accounted for [56,71,107]. The analysis of these models will focus on three critical simulation challenges: elements, boundary conditions, and interactions.

Finite Element Type

Solid elements are the most commonly used element type in the mechanical analysis of bending across all four models [56,71,105,107]. Menard et al. [56], however, incorporate beam and surface elements alongside solid elements to address the computational challenges posed by the large model size and numerous helical wires. The differentiation of wires using solid elements can lead to an overly dense mesh, which is computationally expensive. Inspired by advancements in modelling helical ropes [123], Menard et al. employed a hybrid approach using beam and surface elements to simulate the helical wires effectively. This approach is illustrated in Fig. 21, where beams are meshed using Timoshenko beam elements and the surface, lacking thickness or stiffness, is coupled at the nodes with the beams. This method has been shown to offer a balance between computational efficiency and accuracy [123,124].

In addition to typical commercial FEM program beam elements, special beam elements have been developed for helical wires in flexible structures. Sævik [96] introduced an eight-DOF curved beam element that restricts transverse translation, based on Kirchhoff rod theory [72,73]. This element allows the wire to follow a loxodromic slip path, enhancing the model's fidelity to actual helical behaviours. The numerical program incorporating these elements has been maturely developed and commercialized, as demonstrated in studies by Skeie [125,126], indicating their practical applicability in industry.

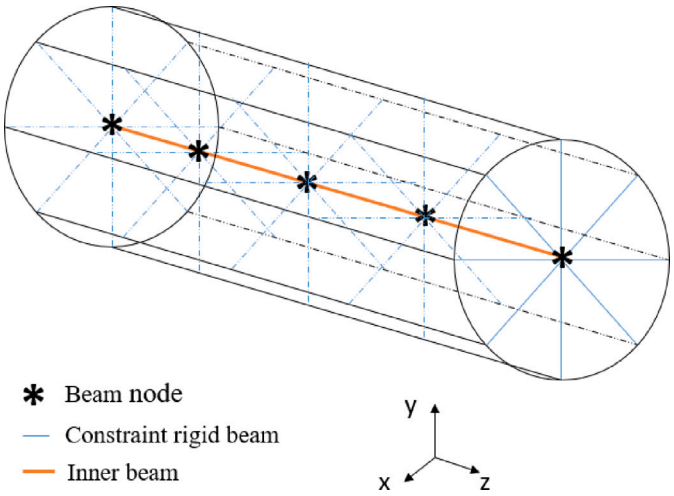

Fig. 21. The combination of beam and surface elements.

Table 10
The friction coefficients and equivalent external pressure used in previous studies regarding flexible structures.

Author	Structure types	Friction coefficient	Equivalent external pressure
Leroy [107]	Three-core SPC	0.15	0
Tyrberg [71]	Three-core SPC	0.25	0.2 MPa
Menard [56]	Three-core SPC	0.2	0.3 MPa
Fang [105]	Single-core SPC	0.12	0
Zhang [130]	Flexible pipe	0.05 – 0.2	1.9 MPa

Contact

Contact in the bending case is more complicated than that in the tension case, not only because both the normal and tangential directions need to be taken into account, but also due to the initial residual stress [30] which is gradually regarded as one of the factors that dominate the stick–slip phenomenon in a multi-lay flexible structure [62,127,128]. Kraincanic [62] made it clear that the initial (manufacturing) interlayer pressures are important for the described analysis and should be given alongside the pipe construction data. Yet this value is hard to obtain directly [30]. Fernando [129] lists methods to measure the value in pressure/tensile armour wires of flexible pipes, for example, by neutron diffraction. The values of the maximum mechanical stress observed in five transmission cables studied by Amyot et al. [87] varied from 4.5 MPa to 6 MPa. However, the initial residual stresses vary everywhere within an SPC, thus in practice, the curvature-bending moment curve from a bending test is recommended to calibrate an equivalent external pressure that imitates the effect from the initial residual stress [30,56]. In the study of other flexible structures, alternatives to deal with the initial residual stress include applying an internal pressure, a tension force or introducing a thermal field that induces radial stresses within the structure [88–90]. Applying external and internal pressure enables the radial stress to propagate among layers. A tension force also generates radial stresses due to the Poisson effect and the existence of helical components, while the expansion induced by thermal variation causes the radial stress by applying a thermal field.

To date, applying an equivalent external pressure is the most popular way that scholars have applied in many flexible structures [56,71,130]. The values given by the previous studies are summarized in Table 10. Notice that out of the four papers about SPCs, Leroy et al. [107] and Tyberg et al. [71] pioneered the simulation of this particular structure, yet they did not provide a bending test to calibrate the equivalent external pressure. Therefore, the equivalent external pressure is not considered in Leroy's work while the value provided by Tybery is out of their industry experiences. It was not until 2023 that Menard et al. [56] first managed to calibrate the equivalent external pressure for a three-core SPC by the curvature-bending moment curve from his bending test, and the value for his SPC is 0.3 MPa. In their work [56], Menard et al. did a sensitivity study of the external pressure on the bending behaviour of the SPC. It is found that when the pressure is set as 0, the curvature-bending moment curve becomes a straight line instead of a hysteresis curve, as shown in Fig. 22. In this case, the components within the SPC directly slip away from each other without the initial stresses that retard the slippage. When the equivalent external pressure increases, the stick section of the curve becomes longer as larger radial stresses introduce larger friction forces that make the slippage more difficult. This phenomenon can also be explained by Eqs. (16) and (20) in the analytical section, which states that the slip curvature and the total moment are affected by the friction coefficient and the contact pressure among the contact interfaces. The same phenomenon was also observed by Zhang et al. [130], who studied a flexible pipe with the test data provided by Witz [131]. Based on the proposed model by Zhang et al. [130], the equivalent external pressure calibrated by the test data on the curvature-bending moment curve is 1.9 MPa, as summarized in Table 10.

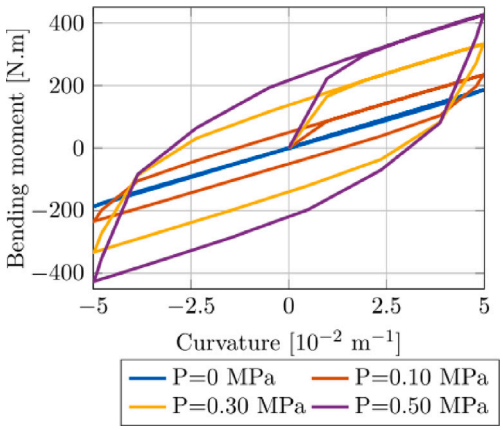

Fig. 22. Evolution as a function of the external pressure on the curvature-bending moment curves [56].

As compared with the tension case, the interaction properties in the tangential direction have received more attention in the bending case. Stick–slip behaviours within flexible structures strongly relate to the contact property in the tangential direction. Coulomb friction is a classical friction method in describing the interaction of contacting surfaces. The model characterizes the frictional behaviour between the surfaces using a coefficient of friction [132] and has been applied in many models [38,55,107,133]. Scholars have also investigated friction methods other than the traditional Coulomb friction method. For example, Dai et al. [134] studied the mechanical behaviour of a flexible pipe by using four different friction models, finding that the pipe exhibits different behaviours. It should be noted that the friction properties are different even in the same flexible structure because the contact interfaces are not the same. For example, the friction coefficients between two polymer interfaces differ from those between polymer and metals. In addition, the friction coefficient can also be affected by many other factors, such as temperature [135], air moisture content [136], etc. Measurement of friction coefficients is also a cumbersome task. Therefore, the structure's equivalent unified friction coefficient is adopted normally.

Another factor affecting contact behaviour is the damping among interfaces [137,138]. Damping in a physical system essentially refers to the loss of energy or, alternatively, energy dissipation. This means the energy is either redistributed to the surroundings or converted into other forms of energy, usually heat, that cannot be recovered. Consequently, this process diminishes the system's motion. Silva [139] classifies the damping sources in mechanical systems as three: internal/material damping, structural damping, and fluid damping. The contact damping among the interfaces here refers to the structural damping that occurs in structural assemblies due to plasticity, dry friction (Coulomb damping), contact and interaction between structural components, typically in joints, connections, supports and other contact surfaces and interfaces. The contact damping itself is a complex subject that receives more and more attention [137,138], however, in the previous studies about multi-layer flexible structures [140,141], the contact damping is merely set as a tool to reduce solution noise and stabilize the structure for numerical consideration. In their studies [140,141], the energy generated by contact damping is extremely tiny as compared to other types of energy, such as the internal energy or strain energy, which means that the contribution of the contact damping in the overall structure can be ignored and the mechanical behaviour is not affected too much by the artificially introduced damping.

Boundary Conditions

When it comes to the boundary conditions, the other problem that comes with it is how to choose a proper length for the bending simulation to eliminate the boundary effects, which is still an open question that no paper gives an explicit answer to. Theoretically, the longer the model, the more the boundary effect is eliminated. However, the contact effect becomes intensive based on the experience from bending tests, and a numerical model with a long length makes a simulation extremely time-consuming. Although full models with a few metres long for flexible pipes that can consider non-uniform curvature along the pipes flourish in the literature [133,142–145], according to the author's review, up until now, there is no a paper exhibiting the simulation details of a 3D bending numerical models same as the sample length in a test for SPCs in the open literature. Researchers are trying to propose reliable and efficient simulation models requiring less computational cost by applying appropriate boundary conditions. Thanks to the periodical structure pattern of helical components, a few numerical models based on the technique of periodical boundary conditions have been proposed [56,71,107].

The technique of periodical boundary conditions can be traced back to the multi-scale analysis, an approach used in various scientific and engineering disciplines to study and model phenomena that occur at multiple scales. It involves analysing a system or process at different levels of detail, from microscale to macroscale, to understand its behaviour comprehensively. Homogenization is a common technique to bridge the different levels of scales where the mathematical tool of asymptotic expansion theory has been adopted frequently. On the macroscale level, SPCs can be regarded as a type of beam-like structures that find significant applications in aerospace engineering, civil engineering, ocean engineering, etc. Helical ropes, lattice, cable-stayed bridges, SPCs, etc., are practical examples. These beam-like structures are characterized by having relatively small dimensions compared to their length. A conventional numerical simulation of these structures leads to heavy computations; therefore, researchers have been

using homogenization theory to finish the simulation by bridging the macroscale beam-like structures to corresponding microscale homogeneous continuous medium.

The theory of the homogenization method applied to slender beam-like structures has been thoroughly developed by Buannic and Cartraud [146,147]. The derived formulas are also used to study slender structures, from simple beam-like structures such as repetitive lattices to more complicated heterogeneous structures such as helical ropes in the past 30 years. More about asymptotic expansion methods for slender structures may be found in Sanchez-Hubert and Sanchez-Palencia, 1992 [148], Trabucho and Viaño, 1996 [149] and Kalamkarov and Kolpakov [150,151]. The periodical boundary conditions derived for slender beam-like structures by Buannic and Cartraudc [146,147] are found in the papers about SPCs during the recent years [56,71,107]. The model length abides by a rule in order to take advantage of the periodical boundary conditions, and it is calculated as:

$$l = k\frac{p_i}{m_i} \tag{21}$$

where $k \in \mathbb{N}$, p is the pitch length, m is the number of helixes, and the index i is the sequence of the current layer. The first two proposed models for SPCs that take advantage of the periodical boundary conditions are given by Tyrberg et al. (2017) [71] and Dupend et al. (2017) [107]. The equations of the periodical boundary conditions in these two papers are quite similar. However, the constitutions of their numerical models differ from each other. Dupend et al. (2017) [107] divided the structure types in the SPC as helical wires and cylinders. The periodical boundary conditions are applied on the helical wires while a new set of constraint equations are derived and applied on the cylinders in order to obtain a constant curvature along the SPC. Besides, the helical shapes of the inner helical components, such as the copper conductors, are not considered and are simplified into straight structures. Tyrberg et al. (2017) [71], instead, choose to consider the inner components' helical configurations. Therefore, his model is much longer, with the inner helical shapes considered based on the length calculated through Eq. (21). The periodical boundary conditions are applied on both sides of the SPC for helical and cylinder components. Both of the models are preliminary, and neither of them gives the curvature-bending moment curves. Their models are not validated by experimental data either.

Very recently, Fang et al. [105] build a RUC model with a length of only 20 mm for the bending study of a single core SPC. A bending test is performed to validate the RUC model. Meanwhile, a full-scale numerical model costing much longer time is used to compare with the RUC model. It is found that the boundary difference between the test and both the two numerical models cause a difference regarding the bending behaviour, although the RUC model agrees well with the full scale model. Ménard, Fabien et al. [56] developed a model for a 3-core SPC based on Tyrberg's work. The helical shapes of the inner conductor cores with longer pitch lengths than the helical wires are considered. A bending test is performed, and the hysteretic curve has been observed through the test and the numerical model.

4.3. Remarks on numerical method

To sum up, the numerical method enables cable designers to gain more insights into the mechanical behaviour of SPCs, particularly at the component level. However, an SPC is too complex to be fully calculated if all details are included in an FEM model. Therefore, the common practice in studying the overall behaviours of SPCs is to simplify the conductors into solid components and ignore the influences of currents and temperature. Even with these simplifications, the computational magnitude remains substantial. To balance accuracy and efficiency in a numerical model, the structure needs to be appropriately simplified. Current numerical analysis mainly focus on bending and tension, with scarce investigation in other loadings such as torsion or compression, let alone combined loading cases. The challenges in constructing the overall model mainly converge into three aspects: establishing the finite element model, dealing with contact issues, and setting proper boundary conditions. The following actions can be taken to balance accuracy and efficiency:

1. Take advantage of special finite elements with fewer degrees of freedom or utilize combined finite elements that generate fewer elements in the simulation.

2. The main challenges in dealing with contact involve initial residual stress and friction coefficient. Typically, an equivalent external pressure is used to mimic the initial residual stress in practice, and an equivalent friction coefficient is employed to simulate friction behaviours within all contact interfaces. If researchers cannot measure the initial residual stress and friction coefficients in their cable sample, they should reference values provided by previous researchers, such as those in Table 10. The equivalent external pressure can range from 0.2–0.3 MPa, and the equivalent friction coefficient in SPC samples typically ranges from 0.12–0.25.

3. Setting up boundary conditions involves selecting the total length of the model. Currently, there is no strict rule on the appropriate length of a model for representing the mechanical behaviours of multi-core SPCs. If cable engineers find the computation too intensive when using full models with a large length, then periodic boundary conditions can help shorten the simulated cable significantly.

5. Conclusions

After introducing the cable configurations, the methods for performing the local mechanical analysis of SPCs, including experimental, analytical and numerical methods, are reviewed. Their advantages and disadvantages are highlighted. While testing is considered fundamental and reliable, the major limitations are that the behaviours at the component level are hard to measure, and combined loading scenarios are hard to imitate in test conditions.

Analytical and numerical methods are two types of analysis methods, drawing on experiences from the oil and gas industry. There are several limitations of current modelling methods on SPCs:

• Most of the current research ignores the influence of inner helical shapes, which might induce a miscalculation of the stiffness and stress.

• The efficiency of a modelling method is infringed if a significant amount of details are considered in order to pursue accuracy.

• Current studies merely focused on individual loadings, and have not stepped into the area where combined loadings are involved.

• Previous researchers have mainly focused on specific types of SPCs, such as single-core or multi-core, but have not established connections between them or developed a model capable of handling both configurations.

• The initial residual stress contributes to the stick–slip behaviour within SPCs, significantly influencing their local mechanical behaviour. Yet, this factor has not been extensively explored.

The practitioners can develop proper modelling methods based on either analytical or numerical methods. The analytical method has its advantage regarding efficiency; however, due to the complexity of SPCs, many assumptions are necessary, and accurately simulating internal mechanical behaviour is challenging. In summary, analytical methods have the following limitations:

1. It is hard to accurately capture the complex contact issue within SPCs.

2. The behaviour of the helical components has not been investigated thoroughly.

The numerical method is a potential way, yet a numerical model becomes too complex to be calculated if it is not built up properly. The efficiency of a numerical model can be enhanced by the following two aspects:

1. Set up appropriate finite elements so that the element number can be reduced.

2. Establish proper boundary conditions to reduce the model size.

One tricky point in developing a numerical method for the local mechanical analysis of SPCs concerns the manipulation of the initial residual stress within contact interfaces. Although this is not fully understood, it has been gradually realized as a crucial factor in influencing especially the bending behaviour. Normally, a curvature-bending moment curve is required to calibrate the equivalent external pressure that imitates the effect from the initial residual stress. The model developers need to take this point in to account.

Apart from the local mechanical analysis of overall SPCs, research on specific components, particularly copper conductors and insulation layers, is also advancing due to their importance within an SPC. Modelling these components requires detailed geometry and often involves multiple physical fields. Although some preliminary numerical models have appeared in the literature, most are still simplified and lack validation by test data. Consequently, there remains significant potential for exploration in future studies.

In general, numerical models offer detailed insights into the physical phenomena involved, potentially reducing material and manufacturing costs while increasing system efficiency and maintaining a substantial safety margin. In the competitive cable market, numerical analysis is considered an essential asset. There is an urgent need to develop an effective numerical model for the local mechanical analysis of SPCs by addressing these challenges, thereby facilitating the design process in the industry.

CRediT authorship contribution statement

Pan Fang: Writing – review & editing, Writing – original draft, Methodology, Investigation, Conceptualization. **Xiao Li:** Writing – review & editing. **Xiaoli Jiang:** Writing – review & editing, Supervision, Conceptualization. **Hans Hopman:** Supervision. **Yong Bai:** Supervision.

Declaration of competing interest

The authors declare the following financial interests/personal relationships which may be considered as potential competing interests: Pan Fang reports financial support was provided by China Scholarship Council [grant number 201906320047].

Acknowledgement

The first author would like to express the gratitude for the support from the China Scholarship Council, China [grant number 201906320047].

Data availability

No data was used for the research described in the article.

References

[1] Herbert GJ, Iniyan S, Sreevalsan E, Rajapandian S. A review of wind energy technologies. Renew Sustain Energy Rev 2007;11(6):1117–45.
[2] Hannan M, Al-Shetwi AQ, Mollik M, Ker PJ, Mannan M, Mansor M, et al. Wind energy conversions, controls, and applications: A review for sustainable technologies and directions. Sustainability 2023;15(5):3986.
[3] Letcher T. Wind energy engineering: a handbook for onshore and offshore wind turbines. Elsevier; 2023.
[4] Zhang Z, Liu X, Zhao D, Post S, Chen J. Overview of the development and application of wind energy in New Zealand. Energy Built Environ 2023;4(6):725–42.
[5] TGS. Global offshore wind farm database and intelligence. 2023, URL https://www.4coffshore.com/windfarms/.
[6] Wind Europe Report. Offshore wind in Europe key trends and statistics 2019. 2019, URL https://windeurope.org/wp-content/uploads/files/about-wind/statistics/WindEurope-Annual-Offshore-Statistics-2019.pdf.
[7] ETIPWind, Roadmap. Roadmap. 2019, ETIPWind, URL https://etipwind.eu/roadmap/.
[8] Insight bottom Prysmian Group. A closer look at 2023 worldwide offshore floating wind market trends. 2023, URL https://www.prysmiangroup.com/en/insight/projects/a-closer-look-at-2023-worldwide-offshore-floating-wind-market-trends.
[9] Hoeser T, Kuenzer C. Global dynamics of the offshore wind energy sector monitored with Sentinel-1: Turbine count, installed capacity and site specifications. Int J Appl Earth Obs Geoinf 2022;112:102957.
[10] Orton H. History of underground power cables. IEEE Electr Insul Mag 2013;29(4):52–7.
[11] Black RM. The history of electric wires and cables, (no. 4). IET; 1983.
[12] CIGRE TB 610. CIGRE TB 610 - Offshore generation cable connections. 2015, URL https://www.researchgate.net/publication/338388640_CIGRE_TB_610_-_Offshore_generation_cable_connections/citations.
[13] Taihan Cable & Solution Co, Ltd. Power generation. 2022, URL https://www.taihan.com/en/business/product/productDetail?idx=20.
[14] NEXANS. Subsea cables | MV medium voltage power & fibre optics cables. 2019, URL https://www.powerandcables.com/subsea-cables-joints-terminations/.
[15] Worzyk T. Submarine power cables: design, installation, repair, environmental aspects. Springer Science & Business Media; 2009.
[16] Ikhennicheu M, Lynch M, Doole S, Borisade F, Wendt F, Schwarzkopf M-A, et al. Review of the state of the art of dynamic cable system design. Brussels, Belgium: COREWIND; 2020.
[17] Hughes B. Power generation. 2020, URL https://www.plasteurope.com/news/SAUDI_ARAMCO_t245063/.
[18] Burke R, Hughes B. Subsea distribution products. 2024, URL https://www.oceaneering.com/subsea-distribution-solutions/products/.
[19] Wang W, Yan X, Li S, Zhang L, Ouyang J, Ni X. Failure of submarine cables used in high-voltage power transmission: Characteristics, mechanisms, key issues and prospects. IET Gener Transm Distrib 2021;15(9):1387–402.
[20] Danikas M, Papadopoulos D, Morsalin S. Propagation of electrical trees under the influence of mechanical stresses: A short review. Eng Technol Appl Sci Res 2019;9(1).
[21] Nasution FP, Sævik S, Gjøsteen JK. Study of fatigue strength of copper conductor considering irregularities surfaces by experimental testings and fe-analysis. In: International conference on offshore mechanics and arctic engineering, vol. 44908. American Society of Mechanical Engineers; 2012, p. 269–75.
[22] Nasution FP, Sævik S, Gjøsteen JK. Fatigue analysis of copper conductor for offshore wind turbines by experimental and FE method. Energy Procedia 2012;24:271–80.
[23] Nasution FP, Sævik S, Berge S. Experimental and finite element analysis of fatigue strength for 300 mm2 copper power conductor. Mar Struct 2014;39:225–54.
[24] WIND EUROPE. The EU offshore renewable energy strategy. 2020, URL https://windeurope.org/policy/position-papers/the-eu-offshore-renewable-energy-strategy/.
[25] TRUST, CARBON. Floating wind joint industry project – phase 2 summary report. 2022, URL https://www.carbontrust.com/our-work-and-impact/impact-stories/floating-wind-joint-industry-programme-jip/floating-wind-jip-phase-ii.
[26] TRUST, CARBON. Floating wind joint industry programme – phase IV summary report. 2022, The Carbon Trust, URL https://www.carbontrust.com/our-work-and-impact/impact-stories/floating-wind-joint-industry-programme-jip/floating-wind-jip-phase-iv.
[27] DNVGL. Subsea power cables for wind power plants. 2020, URL https://www.dnv.com/energy/standards-guidelines/dnv-st-0359-subsea-power-cables-for-wind-power-plants.html.
[28] DNV-RP-F401. Electrical power cables in subsea applications. 2022, URL https://www.dnv.com/oilgas/download/dnv-rp-f401-electrical-power-cables-in-subsea-applications.htm.
[29] Riley C, et al. HV cable qualifications to IEC 62067–2006 and ICEA S-108-720-2004. In: Jicable conf. 2011.
[30] Conseil international des grands réseaux électriquesComité d'études B1. Recommendations for mechanical testing of submarine cables. CIGRÉ; 2015.
[31] Nicholls-Lee R, Thies PR, Johanning L. Coupled modelling for dynamic submarine power cables: interface sensitivity analysis of global response and local structural engineering models. EWTEC; 2021.
[32] Rodabaugh E, George H. Effect of internal pressure on flexibility and stress-intensification factors of curved pipe or welding elbows. Trans Am Soc Mech Eng 1957;79(4):939–48.
[33] McNamara J, O'Brien P, Gilroy S. Nonlinear analysis of flexible risers using hybrid finite elements. 1988.
[34] Ruan W, Chen M, Nie Q, Xu P, Li J, Wang X. Dynamic response of steel lazy wave riser considering the excitation of internal solitary wave and ocean currents. Ocean Eng 2024;294:116708.
[35] Fang P, Jiang X, Hopman H, Bai Y. A review of mechanical analysis of submarine power cables. In: Maritime technology and engineering 5 vol. 2. CRC Press; 2021, p. 559–68.
[36] API. API 17B: recommended practice for flexible pipe. American Petroleum Institute; 2014.
[37] Xu Y, Bai Y, Fang P, Yuan S, Liu C. Structural analysis of fibreglass reinforced bonded flexible pipe subjected to tension. Ships Offshore Struct 2019;14(7):777–87.
[38] Bai Y, Liu T, Ruan W, Chen W. Mechanical behavior of metallic strip flexible pipe subjected to tension. Compos Struct 2017;170:1–10.
[39] Yang Z, Su Q, Yan J, Wu S, Mao Y, Lu Q, et al. Study on the nonlinear mechanical behaviour of an umbilical under combined loads of tension and torsion. Ocean Eng 2021;238:109742.
[40] Lu Q, Chen J, Yang Z, Chao YY, Yue Q. Numerical and experimental analysis of umbilical cables under tension. Adv Compos Lett 2017;26(2):096369351702600205.
[41] Nam W, Chae K, Lim Y. Experimental and theoretical study on the prediction of axial stiffness of subsea power cables. J Ocean Eng Technol 2022;36(4):243–50.
[42] Guo Y, Ye N. Numerical and experimental study on full-scale test of typical offshore dynamic power cable. In: ISOPE international ocean and polar engineering conference. ISOPE; 2020, p. ISOPE–I.
[43] Delizisis P, Dolianitis I, Chatzipetros D, Kanas V, Georgallis G, Tastavridis K, et al. Full scale axial, bending and torsion stiffness tests of a three core HVAC submarine cable. In: International conference on offshore mechanics and arctic engineering, vol. 85147. American Society of Mechanical Engineers; 2021, p. V004T04A009.

[44] dos Santos Paiva MV, Silveira L, Wang H, Hebert CB, Coser TB, López FS, et al. Validation of power cable local stress analysis. In: ISOPE international ocean and polar engineering conference. ISOPE; 2016, p. ISOPE–I.
[45] Witz J, Tan Z. On the axial-torsional structural behaviour of flexible pipes, umbilicals and marine cables. Mar Struct 1992;5(2–3):205–27.
[46] Fang P, Yuan S, Cheng P, Bai Y, Xu Y. Mechanical responses of metallic strip flexible pipes subjected to pure torsion. Appl Ocean Res 2019;86:13–27.
[47] Fang P, Xu Y, Yuan S, Bai Y, Cheng P. Investigation on mechanical properties of fibreglass reinforced flexible pipes under torsion. In: International conference on offshore mechanics and arctic engineering, vol. 51272. American Society of Mechanical Engineers; 2018, p. V07BT06A028.
[48] Bu J, Wang S, Liu W, Ding X. Theoretical prediction for the torsional stiffness of reinforced thermoplastic pipes (RTPs) based on the strain energy-work equivalence of anisotropic cylinders. Ocean Eng 2022;261:112037.
[49] Vaz M, Aguiar L, Estefen S, Brack M. Experimental determination of axial, torsional and bending stiffness of umbilical cables. In: Proceedings of the 17th international offshore & arctic engineering conference, vol. 7. 1998.
[50] Submarine power cables with extruded insulation and their accessories for rated voltages from 6 kv (um=7,2 kv) up to 60 kv (um=72,5 kv) - test methods and requirements. IEC, IEC-63026.
[51] 2H Offshore. Subsea cable failures: What we know and what we don't. 2022, URL https://ore.catapult.org.uk/wp-content/uploads/2022/10/Dynamic-Cable-Technology-Qualification-Oct-2022.pdf.
[52] Karlsen-Husøy KA, Osnes CB, Dwikartika W, Jordal L. On the design of a combined cyclic axial compression and bending test program for a subsea power cable. In: ISOPE international ocean and polar engineering conference. ISOPE; 2024, p. ISOPE–I.
[53] Reda AM, Forbes GL, Al-Mahmoud F, Howard IM, McKee KK, Sultan IA. Compression limit state of HVAC submarine cables. Appl Ocean Res 2016;56:12–34.
[54] Coser TB, Strohaecker TR, López FS, Bertoni F, Wang H, Hebert CB, et al. Submarine power cable bending stiffness testing methodology. In: ISOPE international ocean and polar engineering conference. ISOPE; 2016, p. ISOPE–I.
[55] Tyrberg A, Tjahjanto D, Hedlund J. Bend stiffness of submarine cables—An experimental and numerical investigation. In: Proceedings of the 10th international conference on insulated power cables. 2019.
[56] Ménard F, Cartraud P. A computationally efficient finite element model for the analysis of the non-linear bending behaviour of a dynamic submarine power cable. Mar Struct 2023;91:103465.
[57] Maioli P. Bending stiffness of submarine cables. In: Proceedings of the 9th international conference on insulated power cables. 2015.
[58] Komperød M, Juvik JI, Evenset G, Slora R, Jordal L. Large-scale tests for identifying the nonlinear, temperature-sensitive, and frequency-sensitive bending stiffness of the NordLink cable. In: International conference on offshore mechanics and arctic engineering, vol. 57694. American Society of Mechanical Engineers; 2017, p. V05AT04A004.
[59] Hu H, Yan J, Sævik S, Ye N, Lu Q, Bu Y. Nonlinear bending behavior of a multilayer copper conductor in a dynamic power cable. Ocean Eng 2022;250:110831.
[60] Yan J, Hu H-t, Lu H-l, Yin Y-c, Bu Y-f, Lu Q-z. Experimental study on the influence of cross-section type of marine cable conductors on the bending performance. China Ocean Eng 2022;36(4):629–37.
[61] Skallerud B. Damping models and structural damping in a nonbonded pipe. FPS2000 report, 1991, p. 2.
[62] Kraincanic I, Kebadze E. Slip initiation and progression in helical armouring layers of unbonded flexible pipes and its effect on pipe bending behaviour. J Strain Anal Eng Des 2001;36(3):265–75.
[63] Takahashi I, Masanobu S, Kanada S, Maeda K, Manabe H, Yamaguchi T, et al. Bending tests and cross-sectional analyses of multilayered flexible pipe models. J Mar Sci Technol 2020;25:397–410.
[64] Lukassen TV, Glejbøl K, Lyckegaard A, Berggreen C. Comparison between stress obtained by numerical analysis and in-situ measurements on a flexible pipe subjected to in-plane bending test. In: International conference on offshore mechanics and arctic engineering, vol. 49965. American Society of Mechanical Engineers; 2016, p. V005T04A021.
[65] Sævik S, Ekeberg KI. Non-linear stress analysis of complex umbilical cross-sections. In: International conference on offshore mechanics and arctic engineering, vol. 36118. 2002, p. 211–7.
[66] Lu H, Vaz MA, Caire M, Hernández ID. Full-scale experimental and numerical analyses of a flexible riser under combined tension-bending loading. Mar Struct 2022;86:103275.
[67] Jordal L, Slora R, Vermeer E, Komperod M. A novel bending stiffness rig for identification of subsea cables' and umbilicals' sensitivity to temperature under sinusoidal curvature oscillations. In: ISOPE international ocean and polar engineering conference. ISOPE; 2017, p. ISOPE–I.
[68] Poon CT, Mullins C, Radziunas L, O'Connell E, Connolly A, Leen S. Finite element design study of dynamics in submarine power cables for offshore renewable wind energy. In: International conference on offshore mechanics and arctic engineering, vol. 86618. American Society of Mechanical Engineers; 2022, p. V001T01A023.
[69] Thai H-T, Kim S-E. Nonlinear static and dynamic analysis of cable structures. Finite Elem Anal Des 2011;47(3):237–46.
[70] Chang H-C, Chen B-F. Mechanical behavior of submarine cable under coupled tension, torsion and compressive loads. Ocean Eng 2019;189:106272.
[71] Tjahjanto DD, Tyrberg A, Mullins J. Bending mechanics of cable cores and fillers in a dynamic submarine cable. In: International conference on offshore mechanics and arctic engineering, vol. 57694. American Society of Mechanical Engineers; 2017, p. V05AT04A038.
[72] Kirchhoff G. Über das gleichgewicht und die bewegung eines unendlich dünnen stabes. J Math 1858;291.
[73] Love AEH. A treatise on the mathematical theory of elasticity. University Press; 1927.
[74] Ericksen J, Truesdell C. Exact theory of stress and strain in rods and shells. Arch Ration Mech Anal 1957;1:295–323.
[75] O'Reilly OM. Kirchhoff's rod theory. In: Modeling nonlinear problems in the mechanics of strings and rods: the role of the balance laws. Cham: Springer International Publishing; 2017, p. 187–268. http://dx.doi.org/10.1007/978-3-319-50598-5_5.
[76] O'Reilly OM. Kinematics of rods. 2020, URL https://rotations.berkeley.edu/kinematics-of-rods/.
[77] Dill EH. Kirchhoff's theory of rods. Arch Hist Exact Sci 1992;1–23.
[78] Schlick T. Modeling superhelical DNA: recent analytical and dynamic approaches. Curr Opin Struct Biol 1995;5(2):245–62.
[79] Goyal S. A dynamic rod model to simulate* mechanics of cables and DNA. University of Michigan; 2006.
[80] Goyal S, Perkins NC, Lee CL. Nonlinear dynamics and loop formation in Kirchhoff rods with implications to the mechanics of DNA and cables. J Comput Phys 2005;209(1):371–89.
[81] Yang Y, Tobias I, Olson WK. Finite element analysis of DNA supercoiling. J Chem Phys 1993;98(2):1673–86.
[82] Wang Z, Fratarcangeli M, Ruimi A, Srinivasa A. Real time simulation of inextensible surgical thread using a Kirchhoff rod model with force output for haptic feedback applications. Int J Solids Struct 2017;113:192–208.
[83] Dong L, Qu Z, Zhang Q, Huang Y, Liu G. A general model to predict torsion and curvature increments of tensile armors in unbonded flexible pipes. Mar Struct 2019;67:102632.
[84] Dong L, Zhang Q, Huang Y, Liu G. Slip and stress of tensile armors in unbonded flexible pipes close to end fitting considering an exponentially decaying curvature distribution. Mar Struct 2017;51:110–33.
[85] Knapp R. Derivation of a new stiffness matrix for helically armoured cables considering tension and torsion. Internat J Numer Methods Engrg 1979;14(4):515–29.
[86] Fang P, Jiang X, Hopman H, Bai Y. Mechanical responses of submarine power cables subject to axisymmetric loadings. Ocean Eng 2021;239:109847.

[87] Amyot N, David E, Lee S, Lee I. Influence of post-manufacturing residual mechanical stress and crosslinking by-products on dielectric strength of HV extruded cables. IEEE Trans Dielectr Electr Insul 2002;9(3):458–66.
[88] Wang L, Yue Q. A full layered numerical model for predicting hysteretic behavior of unbonded flexible pipes considering initial contact pressure. Appl Ocean Res 2021;111:102626.
[89] Lu H, Vaz MA, Caire M. A finite element model for unbonded flexible pipe under combined axisymmetric and bending loads. Mar Struct 2020;74:102826.
[90] Wang L, Ye N, Yue Q. A novel helix contact model for predicting hysteretic behavior of unbonded flexible pipes. Ocean Eng 2022;264:112407.
[91] Bournazel C. Calculation of stresses and slip in structural layers of unbonded flexible pipes. 1987.
[92] Feret J, Momplot G. CAFLEX-a program for capacity analysis of flexible pipes. Theory manual. SINTEF structural engineering, report STF71F91019, 1991.
[93] Berge S, Engseth A, Fylling I, et al. FPS2000/flexible risers and pipes: Handbook on design and operation of flexible pipes. Report STF70 A 92006, 1992.
[94] Sævik S. On stresses and fatigue in flexible pipes. 1992.
[95] Kebadze E. Theoretical modelling of unbonded flexible pipe cross-sections [Ph.D. thesis], South Bank University; 2000.
[96] Sævik S. A finite element model for predicting stresses and slip in flexible pipe armouring tendons. Comput Struct 1993;46(2):219–30.
[97] Lukassen TV. Constitutive behavior of tensile armor wires in unbonded flexible pipes. Technical University of Denmark; 2019.
[98] Estrier P. Updated method for the determination of the service life of flexible risers. 1992.
[99] Tan Z, Case M, Sheldrake T. Higher order effects on bending of helical armor wire inside an unbonded flexible pipe. In: International conference on offshore mechanics and arctic engineering, vol. 41979. 2005, p. 447–55.
[100] Larsen C, Saevik S, Qvist J, Fergestad D, Lotveit S. Handbook on design and operation of flexible pipes. In: Joint industry project. 2014.
[101] Sævik S. Theoretical and experimental studies of stresses in flexible pipes. Comput Struct 2011;89(23–24):2273–91.
[102] Sævik S, Li H. Shear interaction and transverse buckling of tensile armours in flexible pipes. In: International conference on offshore mechanics and arctic engineering, vol. 55362. American Society of Mechanical Engineers; 2013, p. V04AT04A013.
[103] Gomes CAPM. Finite element analysis of flexible pipes: Bending combined with tensile load. Universidade Federal do Rio de Janeiro; 2017.
[104] Johansen R, Ekeberg K. Subsea umbilicals-joint industry project aiming to revise ISO 13628-5. In: Offshore technology conference. OTC; 2005, p. OTC–17184.
[105] Fang P, Li X, Jiang X, Hopman H, Bai Y. Bending study of submarine power cables based on a repeated unit cell model. Eng Struct 2023;293:116606.
[106] Fang P, Li X, Jiang X, Hopman H, Bai Y. Development of an effective modeling method for the mechanical analysis of three-core submarine power cables under tension. Eng Struct 2024;317:118632.
[107] Leroy J-M, Poirette Y, Brusselle Dupend N, Caleyron F. Assessing mechanical stresses in dynamic power cables for floating offshore wind farms. In: International conference on offshore mechanics and arctic engineering, vol. 57786. American Society of Mechanical Engineers; 2017, p. V010T09A050.
[108] Ech-Cheikh F, Drissi-Habti M. Numerical modeling of the micromechanics damage of an offshore electrical high-voltage phase. Energies 2023;16(14):5422.
[109] Nasution FP, Sævik S, Gjøsteen JK. Finite element analysis of the fatigue strength of copper power conductors exposed to tension and bending loads. Int J Fatigue 2014;59:114–28.
[110] Jiang K, Bai Y, Cheng P. Fatigue life estimation of stranded copper conductors using the method based on the fatigue damage evolution model. Ships Offshore Struct 2023;1–13.
[111] Miceli M, Carvelli V, Drissi-Habti M. Modelling electro-mechanical behaviour of an XLPE insulation layer for hi-voltage composite power cables: Effect of voids on onset of coalescence. Energies 2023;16(12):4620.
[112] Ech-Cheikh F, Matine A, Drissi-Habti M. Preliminary multiphysics modeling of electric high-voltage cable of offshore wind-farms. Energies 2023;16(17):6286.
[113] Young DG. Predicting failure of dynamic offshore cables by insulation breakdown due to water treeing. The University of Edinburgh; 2020.
[114] Ringsberg JW, Li Z, McCormick R, Fagan N, Stewart G, Marwood T. Structural integrity analysis of marine dynamic cables: Water trees and fatigue. J Offshore Mech Arct Eng 2024;1–57.
[115] Knapp R, Das S, Shimabukuro T. Computer-aided design of cables for optimal performance. Sea Technol 2002;43(7):41–6.
[116] Chae K, Nam W, Shim C. Influence of coiling behavior on axial stress in steel wires of submarine power cables: A numerical study. Ocean Eng 2023;288:116014.
[117] Yoo D-H, Jang B-S, Yun R-H. A simplified multi-layered finite element model for flexible pipes. Mar Struct 2019;63:117–37.
[118] Owolabi G, et al. Critical review of subsea structures in the Gulf of Guinea: "finite element analysis to predict the behaviour of a multi-layer non-bonded flexible pipe under hydrate plug in a static application". 2021.
[119] Timoshenko S, Woinowsky-Krieger S, et al. Theory of plates and shells, vol. 2, McGraw-hill New York; 1959.
[120] Hsieh M-C, Chen B-F, Wang Y, Chang H-C, Liu W-H, Hsu H-L. Determining optimal number of cores in a submarine power cable. Int J Nav Archit Ocean Eng 2022;14:100463.
[121] Bathe K-J. Finite element procedures. Klaus-Jurgen Bathe; 2006.
[122] Reddy JN. Introduction to the finite element method. McGraw-Hill Education; 2019.
[123] Bussolati F. Modèle multi-échelle de la fatigue des lignes d'ancrage câblées pour l'éolien offshore flottant [Ph.D. thesis], Université Paris-Saclay (ComUE); 2019.
[124] Ménard F, Cartraud P. Solid and 3D beam finite element models for the nonlinear elastic analysis of helical strands within a computational homogenization framework. Comput Struct 2021;257:106675.
[125] Skeie G, Sødahl N, Steinkjer O, et al. Efficient fatigue analysis of helix elements in umbilicals and flexible risers: Theory and applications. J Appl Math 2012;2012.
[126] DNV-GL. SESAM white paper–Helica, cross section analysis of compliant structures–flexibles, umbilicals and cables. Hövik, Norway; 2016.
[127] Zhang M, Chen X, Fu S, Guo Y, Ma L. Theoretical and numerical analysis of bending behavior of unbonded flexible risers. Mar Struct 2015;44:311–25.
[128] Ma W, Su L, Wang S, Yang Y, Huang W. Influence of structural parameters of unbonded flexible pipes on bending performance. Ocean Eng 2022;266:113109.
[129] Fernando US, Tan Z, Sheldrake T, Clements R. The stress analysis and residual stress evaluation of pressure armour layers in flexible pipes using 3D finite element models. In: International conference on offshore mechanics and arctic engineering, vol. 37459. 2004, p. 57–65.
[130] Zhang X, Wang S, Ma W, Su L, Yang Y. Study on the influence of bending curvature on the bending characteristics of unbonded flexible pipes. Ocean Eng 2023;281:114730.
[131] Witz J. A case study in the cross-section analysis of flexible risers. Mar Struct 1996;9(9):885–904.
[132] Abaqus V. Documentation. Dassault Systemes Simulia Corporation. 2014. 6.14. 651: 6.2. Belytschko T. & Black T. Elastic crack growth in finite elements with minimal remeshing. Internat J Numer Methods Engrg 1999;45(5):601–20.
[133] Bahtui A, Bahai H, Alfano G. Numerical and analytical modeling of unbonded flexible risers. 2009.
[134] Dai T, Sævik S, Ye N. Friction models for evaluating dynamic stresses in non-bonded flexible risers. Mar Struct 2017;55:137–61.
[135] Wróbel G, Szymiczek M. Influence of temperature on friction coefficient of low density polyethylene. J Achiev Mater Manuf Eng 2008;28(1):31–4.
[136] Feyzullahoglu E, Saffak Z. The tribological behaviour of different engineering plastics under dry friction conditions. Mater Des 2008;29(1):205–11.
[137] Pan W, Li H, Qu H, Ling L, Wang L. Investigation of tangential contact damping of rough surfaces from the perspective of viscous damping mechanism. J Tribol 2021;143(4):041501.
[138] Shi X, Polycarpou AA. Measurement and modeling of normal contact stiffness and contact damping at the meso scale. J Vib Acoust 2005;127(1):52–60.

[139] De Silva CW. Vibration and shock handbook. CRC Press; 2005.
[140] Lukassen TV, Gunnarsson E, Krenk S, Glejbøl K, Lyckegaard A, Berggreen C. Tension-bending analysis of flexible pipe by a repeated unit cell finite element model. Mar Struct 2019;64:401–20.
[141] Lukassen TV, Krenk S, Glejbøl K, Berggreen C. Non-symmetric cyclic bending of helical wires in flexible pipes. Appl Ocean Res 2019;92:101876.
[142] Leroy J-M, Perdrizet Te, Le Corre V, Estrier P. Stress assessment in armour layers of flexible risers. In: International conference on offshore mechanics and arctic engineering, vol. 49132. 2010, p. 951–60.
[143] Perdrizet T, Leroy J, Barbin N, Le-Corre V, Charliac D, Estrier P. Stresses in armour layers of flexible pipes: comparison of abaqus models. In: SIMULIA customer conference. 2011, p. 500–12.
[144] Sertã O, Fumis R, Connaire A, Smyth J, Tanaka R, Barbosa T, Godinho C. Predictions of armour wire buckling for a flexible pipe under compression, bending and external pressure loading. In: International conference on offshore mechanics and arctic engineering, vol. 44908. American Society of Mechanical Engineers; 2012, p. 361–5.
[145] Sævik S, Igland RT. Calibration of a flexible pipe tensile armour stress model based on fibre optic monitoring. In: International conference on offshore mechanics and arctic engineering, vol. 36134. 2002, p. 53–8.
[146] Buannic N, Cartraud P. Higher-order effective modeling of periodic heterogeneous beams. i. asymptotic expansion method. Int J Solids Struct 2001;38(40–41):7139–61.
[147] Buannic N, Cartraud P. Higher-order effective modeling of periodic heterogeneous beams. II. Derivation of the proper boundary conditions for the interior asymptotic solution. Int J Solids Struct 2001;38(40–41):7163–80.
[148] Sanchez-Hubert J, Sanchez-Palencia É. Introduction aux méthodes asymptotiques et à l'homogénéisation: application à la mécanique des milieux continus. Masson; 1992.
[149] Trabucho L, Viano J. Mathematical modelling of rods. In: Handbook of numerical analysis, vol. 4, Elsevier; 1996, p. 487–974.
[150] Kalamkarov AL, Kolpakov AG. Analysis, design and optimization of composite structures, vol. 1, Wiley New York; 1997.
[151] Kolpakov A. Calculation of the characteristics of thin elastic rods with a periodic structure. J Appl Math Mech 1991;55(3):358–65.